J. Fluid Mech. (2010), *vol.* 662, *pp.* 352–383. © Cambridge University Press 2010
doi:10.1017/S0022112010003265

Vortex-induced vibration of a rising and falling cylinder

M. HOROWITZ AND C. H. K. WILLIAMSON†

144 Upson Hall, Cornell University, Ithaca, NY 14853, USA

(Received 30 April 2009; revised 11 June 2010; accepted 12 June 2010;
first published online 19 August 2010)

In this study, we investigate the dynamics of a freely rising and falling cylinder. This is, in essence, a vortex-induced vibration (VIV) system comprising both transverse (Y) and streamwise (X) degrees-of-freedom (d.o.f.), but with zero spring stiffness and zero damping. This problem represents a limiting case among studies in VIV, and is an extension of recent research of elastically mounted bodies having very low spring stiffness, as well as bodies with very low mass and damping. We find that if the mass ratio (where m^* = cylinder mass/displaced fluid mass) is greater than a critical value, $m^*_{crit} = 0.545$, the body falls or rises with a rectilinear trajectory. As the mass ratio is reduced below $m^*_{crit} = 0.545$, the cylinder suddenly begins to vibrate vigorously and periodically, with a 2P mode of vortex formation, as reported in the preliminary study of Horowitz & Williamson (*J. Fluids Struct.* vol. 22, 2006, pp. 837–843). The similarity in critical mass between freely rising and elastically mounted bodies is unexpected, as it is known that the addition of streamwise vibration can markedly affect the response and vortex formation in elastically mounted systems, which would be expected to modify the critical mass. However, we show in this paper that the similarity in vortex formation mode (2P) between the freely rising body and the elastically mounted counterpart is consistent with a comparable phase of vortex dynamics, strength of vortices, amplitudes and frequencies of motion and effective added mass (C_{EA}). All of these similarities result in comparable values of critical mass. The principal fact that the 2P mode is observed for the freely rising body is an interesting and consistent result; based on the previous VIV measurements, this is the only mode out of the known set {2S, 2P, 2T} to yield negative effective added mass ($C_{EA} < 0$), which is a condition for vibration of a freely rising body. In this paper, we deduce that there exists only one possible two degree-of-freedom elastically mounted cylinder system, which can be used to predict the dynamics of freely rising bodies. Because of the symmetry of the vortex wake, this system is one for which the natural frequencies are $f_{NX} = 2f_{NY}$. Although this seems clear in retrospect, previous attempts to predict critical mass did not take this into account. Implementing such an elastic system, we are able to predict vibration amplitudes and critical mass ($m^*_{crit} = 0.57$) for a freely rising cylinder in reasonable agreement with direct measurements for such a rising body, and even to predict the Lissajous figures representing the streamwise–transverse vibrations for a rising body with very small mass ratios (down to $m^* = 0.06$), unobtainable from our direct measurements.

Key words: flow–structure interactions

† Email address for correspondence: cw26@cornell.edu

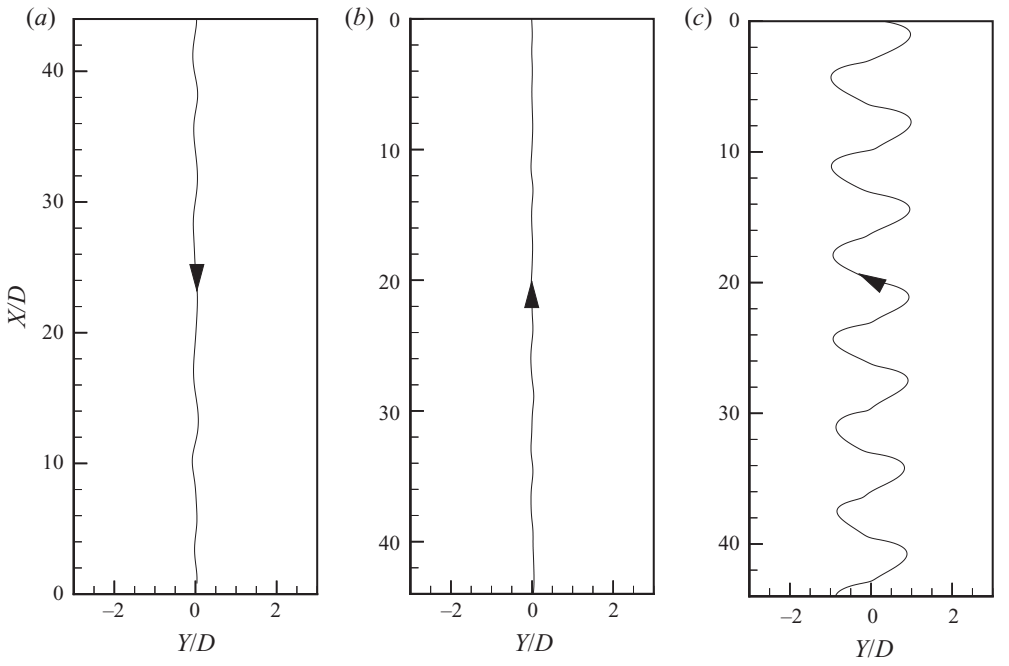

FIGURE 1. Trajectories of freely rising and falling cylinders. (*a*) $m^* = 1.99$, $Re = 9000$; falling cylinders descend rectilinearly. (*b*) $m^* = 0.78$, $Re = 5000$; some rising cylinders can also move with rectilinear trajectories. (*c*) $m^* = 0.45$, $Re = 3800$; a very light rising cylinder exhibits vigorous vibration ($A_Y^* = 1.0$). It should be noted that the Y-axis of these trajectories is significantly expanded relative to the X-axis, so that the non-periodic transient motions in (*a*) and (*b*) are, in reality, extremely small. The trajectories in (*b*) and (*c*) appeared previously in Horowitz & Williamson (2006).

1. Introduction

The problem of vortex-induced vibration (VIV) of cylinders free to move transverse to a free stream has been well studied, and has been presented in a number of reviews (e.g. Sarpkaya 1979; Bearman 1984; Parkinson 1989; Williamson & Govardhan 2004). Regarding our central interest in this paper, the dynamics of rising and falling bodies are relevant to a number of applications. In the case of a freely moving cylindrical body, the question as to whether vibration occurs, and how it occurs, can be of importance in studies of sediment transport, fluidization and other multiphase flows (e.g Richardson & Zaki 1954; Stringham, Simons & Guy 1969; Hartman & Yates 1993), since vibration is known to increase drag as well as heat and mass transfer.

An earlier study of ours in a special issue related to a conference (Horowitz & Williamson 2006) showed that the dynamics of rising and falling cylinders is strongly influenced by the relative density of the body, or what we term here as the mass ratio, m^* (cylinder mass/displaced fluid mass). The main contribution of that work was to determine the critical mass, below which a freely rising or falling body suddenly starts to vibrate periodically at large amplitude, and also to present the vortex formation mode responsible for the large periodic vibration of rising cylinders with sufficiently low mass. The essential points from Horowitz & Williamson (2006) are represented in figures 1 and 2 in this section (somewhat modified from the earlier paper). They began their study with a falling body with mass ratio $m^* = 1.99$. This cylinder, and all other falling cylinders, descend with a straight vertical trajectory, a typical example of which is shown in figure 1(*a*). By removing weight from the body, despite the fact

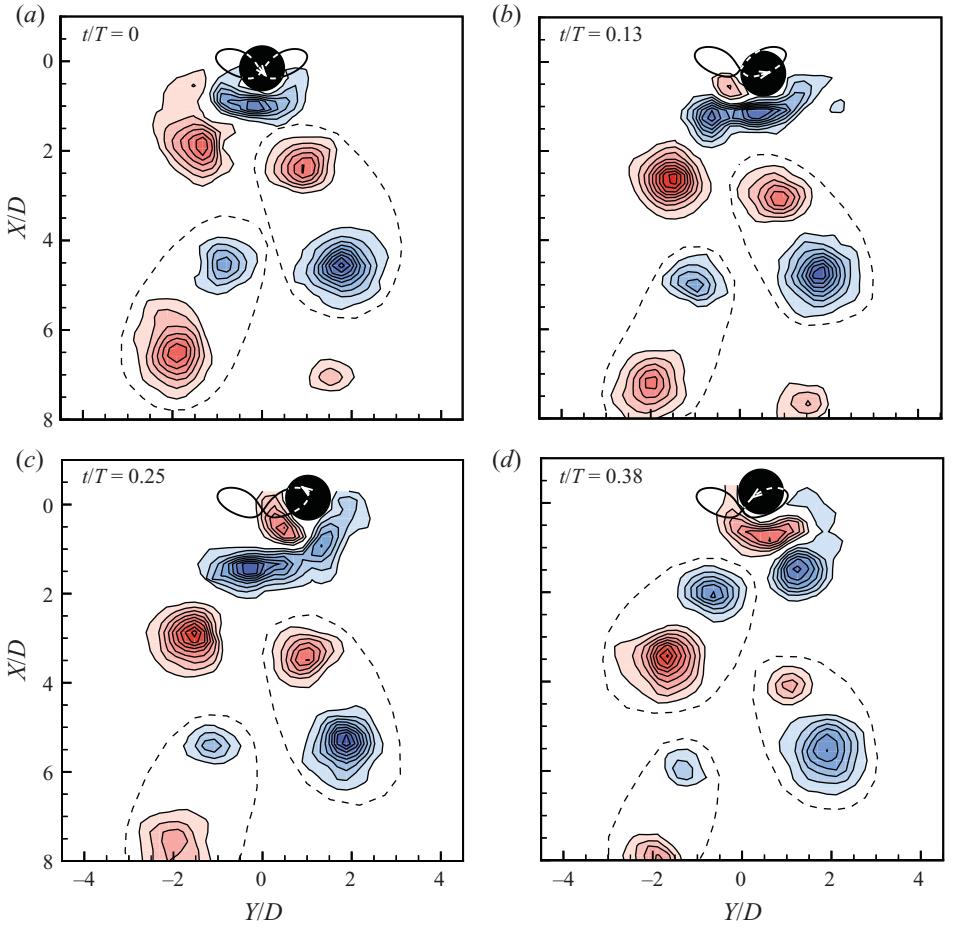

FIGURE 2. A rising cylinder undergoing vibration (in this case $m^* = 0.45$) exhibits the highly periodic 2P vortex formation mode. Each of the plots is separated by an eighth period, combining to show a half-cycle of oscillation. Contour levels are $\omega D/U = \pm\{0.40, 0.80, 1.20, \ldots\}$. $Re = 3800$. The vorticity plot in (d) was shown previously by Horowitz & Williamson (2006).

that the body becomes buoyant, it can still move rectilinearly during its ascent, as shown in figure 1(b) for $m^* = 0.78$. However, by gradually removing mass from the body, they reached a special value of the mass ratio when the body suddenly begins to vibrate vigorously, exhibiting periodic oscillations. The remarkable periodicity of this vibration is seen in figure 1(c), where even fine features of the motion, such as the small kink near the centreline of the trajectory, are visible and highly repeatable in each cycle. A compilation of such measurements in Horowitz & Williamson (2006) yielded the effect of mass ratio on amplitude, demonstrating an abrupt jump between these two states at a critical value $m^*_{crit} = 0.545$. A more developed plot of amplitude versus m^* is presented later in this paper. They went on to uncover the vortex formation mode for freely rising and vibrating bodies, at moderate Reynolds number, finding it to be the 2P mode, comprising two vortex pairs generated per cycle, shown in figure 2. Such a mode is classically found for certain branches of amplitude response for elastically mounted bodies.

In addition to the inherent interest in rising and falling body problems, a freely moving body also represents a special case of an elastically mounted VIV system

with two degrees-of-freedom (d.o.f.), in which there is zero restoring force and zero structural damping (which will be elaborated upon in § 2). In this paper, we will show that by studying a freely rising cylinder, we may deduce the critical mass and dynamics for elastically mounted systems, which would otherwise be difficult to measure using the most conventional VIV experiments. To understand the relationship between these two systems, we must first consider the dynamics of elastically mounted bodies.

In the case of an elastically mounted cylinder undergoing transverse VIV, when the product of the system mass and damping (known as 'mass-damping') is low, three distinct response branches are found as the normalized velocity U^* is increased. These branches are the 'Initial' branch, the 'Upper' branch, where the highest amplitude of vibration occurs, and the 'Lower branch', as defined by Khalak & Williamson (1999). Examples of these different response branches are seen in figure 3. Each branch is associated with a particular mode of vortex formation. (We define the normalized velocity: $U^* = U/f_N D$, where U is the free-stream velocity, f_N is the natural frequency in water and D is the cylinder diameter). The initial branch exhibits a '2S' wake formation mode, employing the nomenclature introduced by Williamson & Roshko (1988), where two single vortices are shed in each cycle of oscillation. The upper and lower branches exhibit a 2P mode, where two vortex pairs are formed per cycle, which is essentially the mode we found for a freely rising cylinder. For a cylinder vibrating transversely with a sinusoidal motion, the resultant wake pattern depends on the normalized amplitude and wavelength (or frequency) of the body motion, as shown by Williamson & Roshko (1988), who mapped the possible wake modes in the amplitude–wavelength plane. (Part of the map of these vortex formation regimes will be found in figure 9.)

Of relevance to the present problem of rising and falling bodies are some previous results concerning the effect of mass ratio (m^* = mass/displaced fluid mass) on the VIV of cylinders. Griffin & Ramberg (1982) and Khalak & Williamson (1999) have shown that reducing the mass ratio increases the range of normalized velocity over which large-amplitude synchronized response occurs. This is illustrated in figure 3 by amplitude response plots for different mass ratios, as a function of normalized velocity U^*, adapted from Govardhan & Williamson (2000). However, by employing the most fundamental parameter $(U^*/f^*)S$, which is equivalent to f_{v0}/f, the ratio of the fixed-cylinder shedding frequency (f_{v0}) to the actual oscillation frequency (f), Khalak & Williamson (1999) demonstrated that for low mass-damping, response data at different mass ratios collapse well, so long as the mass-damping for the data sets is the same (the frequency ratio, f^* and Strouhal number, S are defined in table 1). In the case of the data for $m^* = 1.19$ and 9.31, we find a good collapse of the response data in figure 3(b). The ability to collapse response data at different mass ratios is fortuitous in the case of Y-only cylinder vibration, although we shall see that such collapse is not possible for VIV systems with two d.o.f., whose natural frequencies are the same in both directions. We shall also find that predicting the critical mass is essentially not possible on the basis of elastically mounted cylinder studies, whose natural frequencies in the streamwise and transverse directions are the same.

Before proceeding further, we introduce an equation of motion used to represent the VIV of a cylinder in the transverse direction. In this paper, we define the X direction as parallel to the free stream, and the Y direction as normal to this flow. Bodies able to vibrate with two d.o.f., are denoted as XY-cylinders throughout the paper. The equations of motion used for a Y-cylinder may be written as

$$m\ddot{y} + c\dot{y} + ky = F_Y(t), \tag{1.1}$$

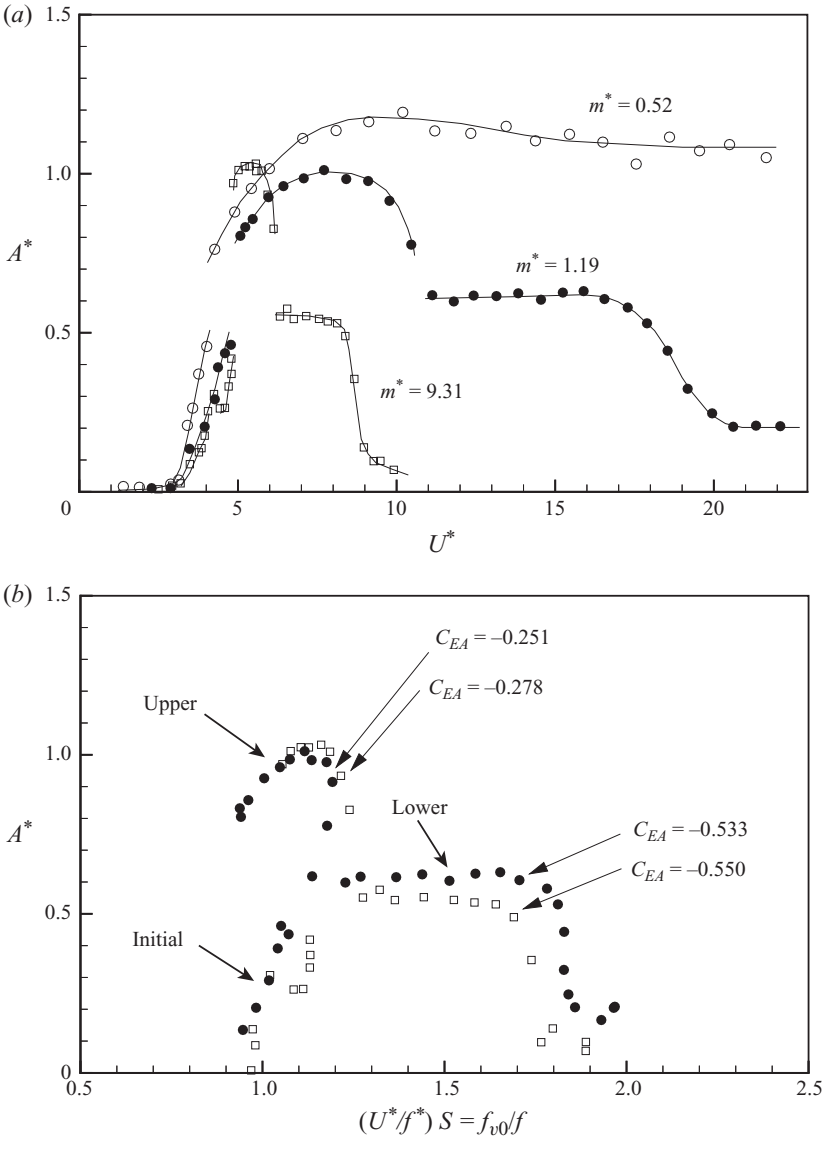

FIGURE 3. Collapse of response data for Y-only cylinders with different mass ratios. (a) Amplitude response at three different mass ratios, from Govardhan & Williamson (2000), with additional unpublished data (from Govardhan & Williamson (2000)). As the mass ratio is reduced, the width of the synchronized response regime increases. For a mass ratio $m^* = 0.52$, large-amplitude oscillations persist to the limit of their facility. □, $m^* = 9.31$; ●, $m^* = 1.19$; ○, $m^* = 0.52$. (b) Response data and C_{EA} at different mass ratios collapse when plotted against the normalized velocity $(U^*/f^*)S$.

where m is the total oscillating structural mass, c is the structural damping and k is the spring stiffness. The displacement, $y(t)$, and fluid force, $F_Y(t)$, have generally, in previous work, been found to be well represented by the sinusoidal functions:

$$y(t) = A\sin(\omega t), \tag{1.2}$$

$$F_Y(t) = F_{Y0}\sin(\omega t + \phi), \tag{1.3}$$

Mass ratio	m^*	$\dfrac{m}{\pi\rho D^2 L/4}$
Damping ratio	ζ	$\dfrac{c}{4\pi f_N(m+m_A)}$
Equivalent damping ratio	ζ_{eq}	$\dfrac{c}{4\pi f_{v0}(m+m_A)}$
Normalized velocity	U^*	$\dfrac{U}{f_{NY}D}$
Amplitude ratios	A_Y^* A_X^*	$\dfrac{A_Y}{D}$ $\dfrac{A_X}{D}$
Frequency ratios	f_Y^* f_X^*	$\dfrac{f_Y}{f_{NY}}$ $\dfrac{f_X}{f_{NX}}$
Force coefficients	C_Y C_X	$\dfrac{F_Y}{\frac{1}{2}\rho U^2 DL}$ $\dfrac{F_X}{\frac{1}{2}\rho U^2 DL}$
Effective added mass	C_{EAY} C_{EAX}	$\dfrac{C_Y\cos\phi_Y}{2\pi^3 A_Y^*}\left(\dfrac{U^*}{f_Y^*}\right)^2$ $\dfrac{C_X\cos\phi_X}{2\pi^3 A_X^*}\left(\dfrac{U^*}{f_X^*}\right)^2$
Reynolds number	Re	$\dfrac{\rho U D}{\mu}$

TABLE 1. Non-dimensional groups for an elastically mounted two degree-of-freedom cylinder in VIV. The added mass, m_A, is given by $m_A = C_A m_d$, where m_d is the displaced fluid mass, and C_A is the potential added-mass coefficient ($C_A = 1.0$ for a circular cylinder). In the above groups, f_N = still-water natural frequency, D = cylinder diameter, L = cylinder length, ρ = fluid density, U = free-stream velocity, μ = viscosity. For simplicity, in various locations in the text, the subscript 'Y' may sometimes be omitted; in this case, the parameters are assumed to be in the transverse direction.

where $\omega = 2\pi f$, with f being the oscillation frequency, and ϕ is the phase angle between the fluid force and cylinder displacement. From equations (1.1)–(1.3), and using the non-dimensional parameters defined in table 1, we derive expressions for the amplitude and frequency of the cylinder response:

$$A^* = \frac{1}{4\pi^3}\frac{C_Y\sin\phi}{(m^*+C_A)\zeta}\left(\frac{U^*}{f^*}\right)^2 f^*, \tag{1.4}$$

$$f^* = \sqrt{\frac{m^*+C_A}{m^*+C_{EA}}}, \tag{1.5}$$

where C_A is the potential added mass coefficient ($C_A = 1.0$ for a circular cylinder), and C_{EA} is an effective added mass coefficient proportional to the force, due to the vortex dynamics, that is in phase with the body acceleration:

$$C_{EA} = \frac{C_Y\cos\phi}{2\pi^3 A^*}\left(\frac{U^*}{f^*}\right)^2. \tag{1.6}$$

Although the effect of the mass ratio on the width of the synchronization regime (in a plot of response versus normalized velocity) has been observed before, Govardhan & Williamson (2000) found that for a cylinder with very low mass, $m^* = 0.52$, the

synchronized large-amplitude response persisted beyond the maximum speed limits of their facility, and appeared as if it would continue indefinitely, as may be seen in figure 3(*a*). Using response data for a variety of cylinders with different mass ratios, they deduced an equation for the oscillation frequency in the lower response branch,

$$f^*_{lower} = \sqrt{\frac{m^* + C_A}{m^* - 0.54}}. \tag{1.7}$$

One may see immediately that this frequency equation suggests that for mass ratios less than a certain critical value, $m^*_{crit} = 0.54$, the frequency ratio f^* is not defined. Effectively this means that the lower branch of response cannot be reached and will not exist. Instead, they predicted that large-amplitude synchronized vibration (on the upper response branch) would occur over an infinitely wide regime of normalized velocities ($U^* \to \infty$), thus suggesting why the response at $m^* = 0.52$ persists to high velocities.

Subsequently, Govardhan & Williamson (2002) developed a simple experiment that allowed them to determine the dynamics of a cylinder at infinite normalized velocity, allowing the critical mass to be found directly. The natural frequency f_N of the system was set to zero by removing the springs (i.e. setting $k = 0$), resulting in infinite $U^* = U/f_N D$. Under these conditions, by gradually removing mass from the system, they accurately deduced that for mass ratios exceeding a critical value, $m^*_{crit} = 0.542$, the cylinder exhibited negligible vibration, but upon reaching this value, the cylinder would suddenly begin to oscillate vigorously, in excellent agreement with the predictions of a critical mass by Govardhan & Williamson (2000). These results are directly relevant to the problem of rising and falling bodies we study here, as will be seen later.

We shall now turn to the case of a cylinder vibrating in both the transverse (Y) and streamwise (X) directions, which arises in many practical cases of cylinders undergoing VIV, such as riser tubes or heat exchangers. This is of relevance here, because our freely rising and falling body can vibrate horizontally (Y) and vertically (X) as it travels through the fluid. One may note that the addition of a streamwise degree of freedom might be expected to influence the fluid forces acting on the cylinder, which determine the critical mass through the parameter C_{EA}. This leads us to ask: does a critical mass exist for an unrestrained cylinder in two d.o.f. – one for which there is no stiffness or damping in both transverse and streamwise directions?

Despite the large amount of work on cylinders undergoing purely transverse VIV, there have been relatively few studies that have considered the VIV of an elastically mounted cylinder in two d.o.f. (in XY motion). Early studies of such XY cylinders were performed by Moe & Wu (1990) and Sarpkaya (1995), but with different mass ratios in the transverse and streamwise directions. The present work, however, will examine only the case where the mass ratio is the same in both directions, corresponding to most practical examples of XY systems.

Jauvtis & Williamson (2004) studied an elastically mounted XY cylinder using a pendulum apparatus that allowed an identical oscillating mass and natural frequency in both directions. They found that for mass ratios above $m^* = 6$, the XY response exhibited the same branches as the transverse-only case, with similar transverse amplitudes, and very little streamwise motion. However, at lower mass ratios ($m^* = 2.6$–4, and possibly lower m^*), they found that the upper branch is replaced by a 'super-upper' branch, characterized by very large amplitudes of around 3 diameters peak-to-peak ($A^*_Y \sim 1.5$) and a wake comprising two triplets of vortices formed in

each cycle, defined as a '2T' mode. (The super-upper response branch is included later in figure 9*b*, along with the initial and lower branches from Jauvtis & Williamson 2004). The streamwise amplitudes in the super-upper branch are significant ($A^*_X \sim 0.3$), generating trajectories with a pronounced figure-of-eight or crescent shape, while in the initial and lower branches the streamwise motion is much smaller ($A^*_X \sim 0.05$). A three-branch response with comparable peak amplitudes was found by Dahl, Hover & Triantafyllou (2006) for a system with slightly different transverse and streamwise mass ratios and $f_{NX}/f_{NY} = 1$. Using controlled vibration, Jeon & Gharib (2001, 2004) have shown that the vortex dynamics behind an XY cylinder are sensitive not only to the streamwise amplitude, but also to the phase, θ, between the transverse and streamwise oscillations. This is quite relevant to our results presented later.

The results of these studies indicate that the vortex formation modes and forces exerted on a cylinder may be significantly affected by streamwise vibration, and would be expected to impact the value of the critical mass. Interestingly, Jauvtis & Williamson (2004), considering the lower branch frequency equation (defined in (1.7)) in the same manner as Govardhan & Williamson (2000), deduced a critical mass of $m^*_{crit} = 0.52$, which is close to the value for a Y-only motion cylinder. Their arrangement comprised a spring system giving the same natural frequencies in the X and Y directions ($f_{NX} = f_{NY}$). On the other hand, Aronsen (2007) performed a set of XY controlled vibration experiments where he found very large $-C_{EAY}$, from -1.5 to -7 in regions where fluid excitation is positive, and hence where free vibration is expected to occur. This result suggests that the critical mass of an XY cylinder could be an order of magnitude greater than predicted by Jauvtis & Williamson (2004) – as high as $m^*_{crit} = 7$. However, in § 2 of the present paper, we will show that such predictions are not necessarily accurate, due to the fact that unlike the Y-only case, the XY cylinder response does not collapse with mass-damping alone, but is also affected independently by the mass ratio. Consequently, in order to predict a critical mass using elastically mounted data, experiments (where $f_{NX} = f_{NY}$) would need to be performed at mass ratios close to the value of the critical mass itself (the work of Jauvtis & Williamson 2004 was only able to reach a minimum mass of $m^* = 2.6$, given their pendulum experimental arrangement); it cannot be predicted on the basis of response plots for higher mass ratios, in the manner of Govardhan & Williamson (2002).

Rather than set out to perform these elastically mounted experiments, we approach the problem in a very different way. We shall use freely rising and falling bodies to find the critical mass. In essence, we show in § 2 that freely rising and falling cylinders are equivalent to a two-d.o.f. VIV cylinder with no restoring force in either direction of motion. Of course, this trivial statement is obvious; however, this fact is pointed out because it does allow us to determine accurately the critical mass that is applicable to 'restrained' two-d.o.f. cylinders, just as we were able to do in the one-d.o.f. case (Govardhan & Williamson 2002). This may seem like an obvious course to follow, but it has not been done before, and neither has a link between rising and falling bodies and elastically mounted experiments been made before (with the exception of Horowitz & Williamson 2006).

Although there have been numerous studies of the dynamics of rising and falling bodies, almost none have focused on circular cylinders. Most investigations have considered spherical or ellipsoidal shapes, like bubbles (see the classic text by Clift, Grace & Weber 1973, or the review of Magnaudet & Eames 2000), or solid spheres (e.g. Jenny, Dušek & Bouchet 2004; Veldhuis *et al.* 2005; Horowitz & Williamson 2008, 2010). In addition, much of the work on cylindrical bodies has considered the

case of disks or very flat cylinders, as in the studies of Willmarth, Hawk & Harvey (1964) and Fernandes *et al.* (2007).

For cylinders with larger aspect ratios ($L/D =$ length/diameter), experiments by Marchildon, Clamen & Gauvin (1964), Jayaweera & Mason (1965), Isaacs & Thodos (1967) and Stringham, Simons & Guy (1969) have shown that freely falling cylindrical particles undergo pitching motions about the midpoint of their span over a wide range of Reynolds numbers ($Re = 200$–$60\,000$). Jayaweera & Mason (1965) and Isaacs & Thodos (1967) found that the amplitude of the pitching oscillations decreased as the cylinder aspect ratio increased, so that sufficiently long cylinders fell steadily, without pitching vibration.

In addition to pitching oscillations, additional types of motion have been observed. For $Re > 8000$, Stringham *et al.* (1969) found a yawing oscillation about a vertical axis through the centre of the cylinder that was superposed on the pitching motion, while Marchildon *et al.* (1964) found periodic motion in a direction parallel to the cylinder length that was synchronized with the pitching oscillations. Finally, at low Reynolds numbers there are some studies of freely falling cylinders, some of which are related to sedimentation. Feng, Hu & Joseph (1994) and Hu (1995) have studied falling cylinders, finding that they sometimes move quite periodically, but can also fall with irregular, non-periodic lateral motion, depending on Re and wall effects.

The types of pitching, yawing or surging dynamics for free cylinders at moderate Re, mentioned above, are not observed in our experiments, where we have restrained our cylinder between a set of false walls, with a narrow gap between each wall and the ends of the cylinder. This ensures that the cylinder remains horizontal (without pitching) and without motion parallel to the longitudinal axis. No previous studies exist, to our knowledge, concerning free cylindrical bodies under such conditions (with the exception of a preliminary paper Horowitz & Williamson 2006). As stated earlier, this problem is a limiting case of classical VIV studies for cylinders, and represents the case of a two degree-of-freedom elastically mounted XY cylinder, in the limit of zero spring stiffness in both the X and Y directions.

We shall show in § 2, that the freely vibrating cylinder, under the effect of a net buoyancy force, is directly equivalent to a two-d.o.f. (XY) cylinder, whose spring stiffness and damping have been removed. This will allow us to determine conditions for vibration of a freely rising or falling body, and provides a means to determine the critical mass for an XY system. Details concerning our experimental approach are given in § 3. A preliminary paper (Horowitz & Williamson 2006) showed that the critical mass for the rising cylinder, is given as: $m^*_{crit} = 0.545$, and that the large-amplitude vibration below this mass, was associated with the 2P mode of vortex formation. In § 4, we indicate that the critical mass is similar to the critical mass for a Y-only elastically mounted cylinder, at comparable Reynolds numbers, despite the presence of streamwise vibration. We present regimes of vibration or straightline trajectories for rising or falling cylinders in the plane of m^* versus Galileo number, or m^* versus Reynolds number.

In § 5, we find that the similarity in vortex formation mode, namely the 2P mode, between the freely rising body and the corresponding elastically mounted case (with Y motion only), is consistent with a comparable phase of vortex dynamics and vortex strengths, as well as comparable amplitudes and frequencies of transverse motion. Finally, we find a similar effective added mass (C_{EA}). All of these similarities result in comparable values of critical mass. Compared with elastically mounted XY cylinders,

freely rising cylinders exhibit larger streamwise amplitudes, and markedly different phase between streamwise and transverse motion. In § 6, we employ a special case of an elastically mounted XY cylinder arrangement. It is remarkable that in fact, such an elastically mounted system, where the natural frequencies in the X and Y directions are related by $f_{NX} = 2f_{NY}$, is equivalent to a freely rising and falling cylinder experiment, and we may therefore use such a system to predict rising and falling dynamics, over a range of mass ratios, down to values not physically possible with our experimental facilities. In retrospect, such an approach may seem essential, but past efforts to determine critical mass for two d.o.f., did not take such a required frequency ratio into account This is discussed, along with predictions that are quite comparable to the freely rising body, in § 6. Conclusions are presented in § 7.

2. Predicting critical mass using elastically mounted cylinders

In their elastically mounted experiments, Govardhan & Williamson (2000) were able to predict the critical mass for a cylinder under transverse-only motion, which was in excellent agreement with the value measured directly for cylinders with no restoring force (Govardhan & Williamson 2002). These elastically mounted experiments can be implemented to successfully make such predictions, even if the critical mass is distinctly below the mass ratio used in the elastically mounted set-up. To understand this fact, it is necessary to consider the cylinder response in the frequency–amplitude plane, where there is a collapse of response data for constant values of mass-damping; i.e. there is no independent variation of the response plot with variation of mass (over the wide range of mass-damping values studied in Khalak & Williamson 1999; Govardhan & Williamson 2000). We shall further explain that the same predictive procedure is not possible for a system with two d.o.f., where $f_{NX} = f_{NY}$, because the response in this case is indeed affected by independent variation of mass ratios. In essence, to find the critical mass for an XY cylinder, one has to actually conduct an experiment very close to what in hindsight turns out to be the critical mass.

The response of a system with a particular mass ratio and damping, and no restoring force, corresponds to a single point in the frequency–amplitude $\{f_{v0}/f, A^*\}$ plane, which we refer to as the 'operating point' of the system, in this paper. To show how the operating point is determined, we consider the equation of motion for a cylinder vibrating without springs. With $k = 0$, the amplitude and frequency equations (1.4)–(1.5) become

$$A^* = \frac{C_Y \sin\phi}{4\pi^3(m^* + C_A)\zeta_{eq}} \left(\frac{f_{v0}}{f}\right) \frac{1}{S^2}, \tag{2.1}$$

$$m^* + C_{EA} = 0. \tag{2.2}$$

The operating point for a system with a given mass (m^*) and damping (ζ) is the point in the $\{f_{v0}/f, A^*\}$ plane that is a solution to both equations (2.1) and (2.2). As an example, we consider the case of a system with zero damping, shown schematically in figure 4. For zero damping, the amplitude equation is satisfied on a contour in the frequency–amplitude $\{f_{v0}/f, A^*\}$ plane where the fluid excitation is zero, $C_Y \sin\phi = 0$. This 'zero-excitation contour' may be determined using controlled vibration data sets, such as those of Hover, Techet & Triantafyllou (1998) or Morse & Williamson (2009*b*,*c*), and is also represented very closely by the response data of a cylinder undergoing free vibration at low mass-damping. An operating point exists if the frequency equation, $C_{EA} = -m^*$, is satisfied somewhere on the zero-excitation contour,

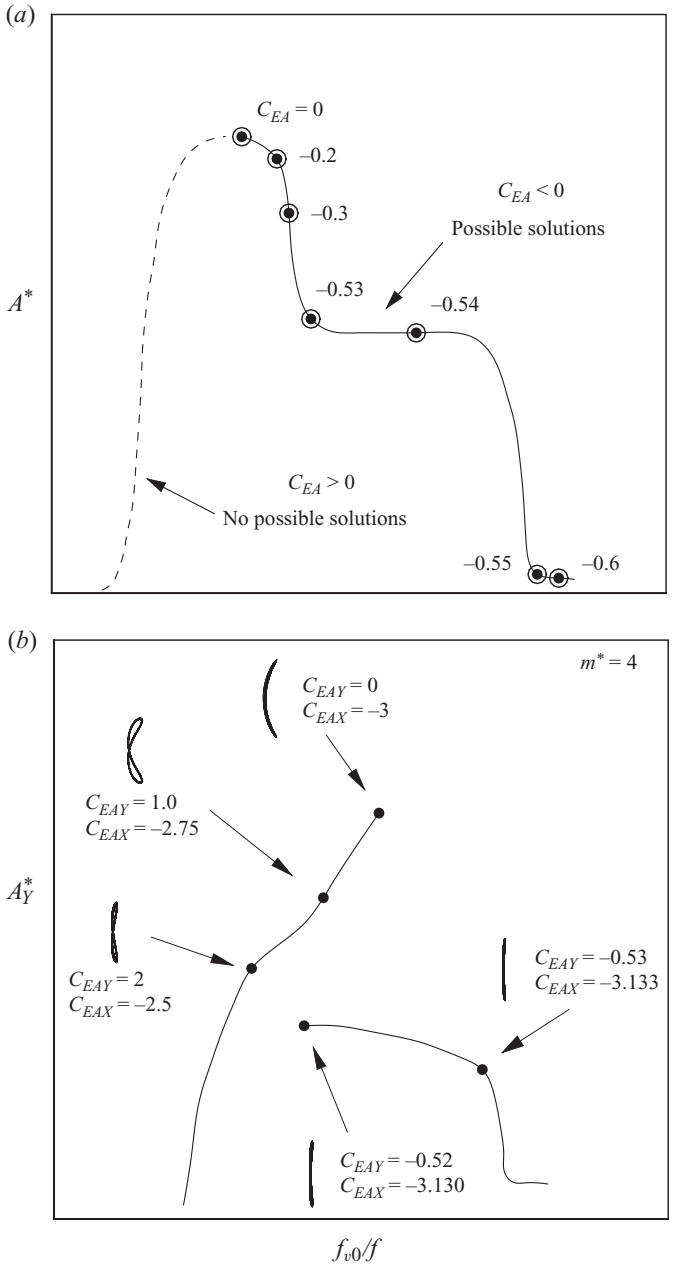

FIGURE 4. (*a*) Schematic showing operating points for the *Y*-only cylinder, which correspond to different values of C_{EA} on the zero-excitation contour. —, $C_{EA} < 0$, operating points exist; - - -, $C_{EA} > 0$, no operating points can exist; ◉, examples of possible operating points. (*b*) Predicting operating points for cylinders with two d.o.f. Schematic of a typical zero-excitation contour for an *XY* cylinder with mass ratio $m^* = 4$, based on data from Jauvtis & Williamson (2004). Pairs of (C_{EAY}, C_{EAX}) are shown at various locations (●), along with the shape of the corresponding Lissajous figures showing the shape of the *XY* motion. No possible operating points exist.

since both equations (2.1) and (2.2) must be satisfied together. Since m^* is positive, this can only occur where C_{EA} is negative. For typical values of C_{EA} from experimental data, schematically shown in figure 4, vibration of an unrestrained cylinder will occur for mass ratios up to $m^*_{crit} = [-C_{EA}]_{max} = 0.54$. For heavier bodies, $m^* > m^*_{crit}$, no solutions are found to yield a significant and periodic response amplitude.

We recall from figure 3(*a*) that decreasing the mass ratio for an elastically mounted *Y*-cylinder dramatically increases the regime of U^* over which large-amplitude vibration occurs. We see in figure 3(*b*) that by replotting the data with the parameter $(U^*/f^*)S = f_{v0}/f$, there is a good collapse of the response for constant mass-damping. As shown from the two pairs of C_{EA} data in figure 3(*b*), not only is the amplitude collapsed but also the values of effective added mass, C_{EA}. If however, the response plot shape were to change as mass is independently varied, then one could not predict values of amplitude or $-C_{EA}$ accurately, even if mass-damping is kept constant. This is the case with the two-d.o.f. *XY* motion (with $f_{NX} = f_{NY}$), where below about $m^* = 6$, mass independently changes the observed response branches (Jauvtis & Williamson 2004), and thereby also changes the values of $-C_{EA}$ yielding the critical mass.

Vibration studies for bodies in *XY* motion have shown that the freedom to vibrate in the streamwise direction can have a significant effect on the response, and on the vortex dynamics of the system, which could profoundly affect the critical mass. We may set out to find the critical mass for an *XY* cylinder using response data from existing *XY* experiments to predict operating points, following the same predictive procedure as for the transverse-only cylinder. If the system has no restoring force in both the *X* and *Y* directions, and no damping, we find

$$C_Y \sin\phi_Y = C_X \sin\phi_X = 0, \tag{2.3}$$

$$C_{EAY} = C_{EAX} = -m^*, \tag{2.4}$$

where C_Y, C_X, C_{EAY} and C_{EAX} are defined in table 1.

These equations may be used to determine operating points in the plane of amplitude A^* and frequency f_{v0}/f. In figure 4(*b*), we consider a schematic of an *XY* response with $m^* = 4$ and zero damping, based on data from Jauvtis & Williamson (2004), where $f_{NX} = f_{NY}$. Immediately one notes that nowhere are there matching values of C_{EAX} and C_{EAY} – they are markedly dissimilar throughout the response plot, thus the data for $m^* = 4$ suggest that no critical mass may be found. However, in the *XY* case, the response is indeed influenced independently by the variation of mass; a different response plot shape emerges with each change of mass ratio m^*, and therefore there is the possibility that at some small enough mass, $C_{EAX} = C_{EAY} < 0$ will arise somewhere on the response plot to yield operating points for an unrestrained cylinder and also a value of the critical mass.

We now show that a single set of response data, even at very low mass ratios, can never be used to predict the critical mass. For an elastically mounted system with $f_{NX} = f_{NY}$, C_{EAX} and C_{EAY} are related according to

$$C_{EAX} = \tfrac{1}{4} C_{EAY} - \tfrac{3}{4}(m^*). \tag{2.5}$$

This relation, derived from the frequency equations in the *X* and *Y* directions, depends explicitly on the mass ratio of the system. Therefore, as a direct result of the equations of motion, one would not expect collapse of C_{EAX} and C_{EAY} over any range of mass ratios, and no single set of response data could be used to predict a critical mass. At most, one elastically mounted response plot could predict a single operating point, while estimating a critical mass would require knowledge of all operating points. The

one operating point would occur where (2.5) satisfies $C_{EAX} = C_{EAY}$. This can only happen if $C_{EAX} = C_{EAY} = -m^*$, so, as expected, a set of elastically mounted response data at one mass ratio cannot provide information about an unrestrained body at any other mass ratio.

The requirement that $C_{EAX} = C_{EAY}$ at an operating point is the cause of the wide variation in reported critical mass values for an XY cylinder, ranging from $m^*_{crit} = 0.52$ to $m^*_{crit} = 7$. As discussed above, response data from Jauvtis & Williamson (2004) do not contain any points where $C_{EAX} = C_{EAY}$, and cannot predict the critical mass. Likewise, Aronsen (2007) had the same misconception in his predictions using controlled vibration experiments, finding high values of $-C_{EAY} = 1.5$–7 in regions of positive energy transfer from the fluid to the body. However, because his lowest value of C_{EAX} was -0.2, the motions generating these very large negative C_{EAY} could not have corresponded to operating points of an unrestrained body.

Since we are interested in the behaviour at infinite normalized velocity U^*, one may consider removing the spring stiffness from the system (giving $k = 0$). In this manner, the critical mass could be measured directly. For a two-d.o.f. (XY) system this would mean not only removing the springs in the transverse direction (as implemented by Govardhan & Williamson 2002) but also removing the springs in the streamwise direction. This is simply not possible, because the springs in the streamwise direction are essential to provide a mean force (proportional to the mean spring deflection, $\bar{x}$) to balance the mean drag, $\bar{F}_X$, according to $k\bar{x} = \bar{F}_X$. Without this force, the cylinder would get carried off downstream with the flow! In the case of a freely rising cylinder, there exists such a mean force, namely, the net buoyancy, $|B - W|$, which is equal to the mean drag: $|B - W| = \bar{F}_X$. Consequently, the freely rising and falling body is equivalent to the two-degree-of-freedom system, but with no damping and no spring stiffness. Of course, this could be seen as a trivial statement, in retrospect, but in fact this case is relevant to restrained bodies, in that it yields directly the critical mass for such elastically mounted bodies.

3. Experimental details

Our rising and falling cylinder experiments are performed in a vertical tank, shown schematically in figure 5. This experimental arrangement has also been described in Horowitz & Williamson (2006), where some preliminary results were shown. The tank has dimensions $0.4\,\mathrm{m} \times 0.4\,\mathrm{m} \times 1.5\,\mathrm{m}$, and is filled with water with a kinematic viscosity $\nu = 0.95 \times 10^{-6} \pm 0.02 \times 10^{-6}$ m^2 s^{-1}. A set of vertical false transparent walls are placed inside the tank, aligned to be precisely parallel to each other. The cylinder, with diameter, $D = 1.91$ cm or $D = 2.54$ cm, and length, $L = 35.3$ cm, is placed horizontally to span the full width between the false walls (allowing a small gap of the order of 10^{-3} m on either side). This enabled motion in transverse and streamwise directions, but without pitching or movement in the direction of the cylinder axis. Any tendency for the cylinder to pitch occurred only immediately after its release, prior to it reaching its steady state motion. The close proximity to the walls ensured that such nascent pitching motions were not allowed to grow, resulting in steady-state motion in the X and Y directions only. The gap did not affect the cylinder dynamics, provided that the cylinder is launched with reasonable care, as described below, to prevent rubbing against the false walls.

Buoyant cylinders are held in place at the bottom of the tank using a rubber-coated hook and electromagnets. The hook would hold the cylinder after its insertion in the tank, while the water settled for around an hour. Several minutes before running

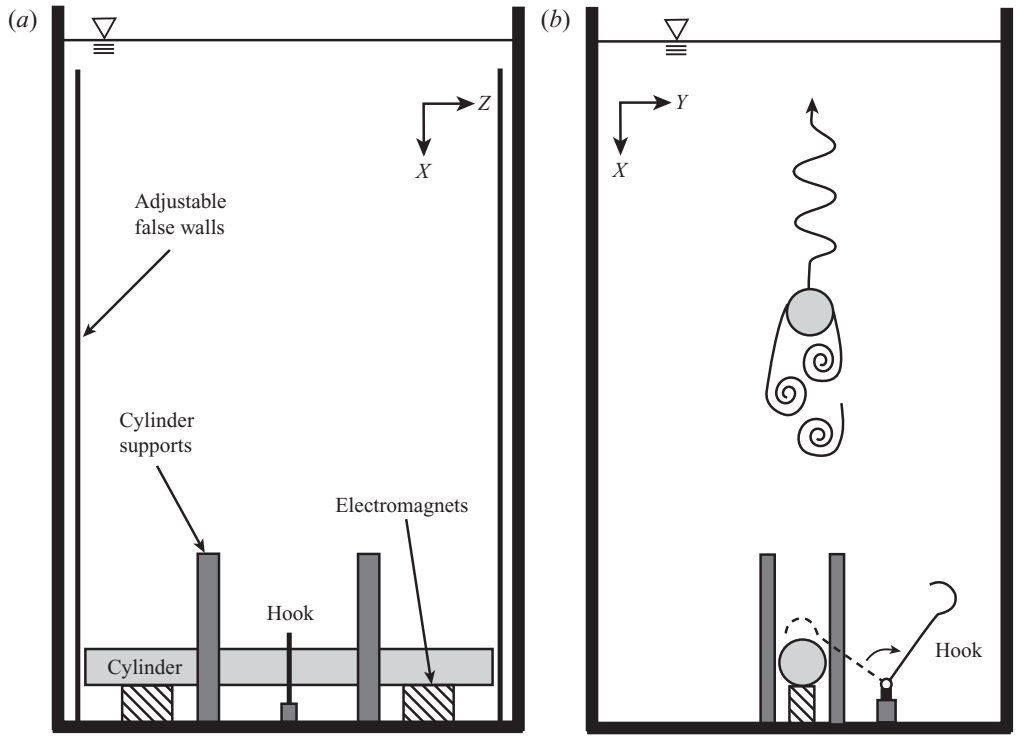

FIGURE 5. Schematic of the experimental facility, shown in a view normal to the length of the cylinder (*a*) and along the length of the cylinder (*b*).

an experiment, the hook was removed, and the electromagnets were used to hold the cylinder before its release. This allowed for a smoother launch of the cylinder than could be achieved using the hook alone. The magnets were not used for longer durations, as they heated up slightly after some minutes, possibly causing small local convection currents in the tank that could have affected initial transient dynamics. For falling cylinders, the launching apparatus could be inverted and placed at the top of the tank. The cylinder used in this study is hollow, and empty of water, allowing its mass ratio to be altered by adding or removing a number of small weights centrally placed within its interior. The added weight was carefully distributed symmetrically around the cylinder's longitudinal axis, and symmetrically with respect to the centre of the span. After adding weight, the cylinder was sealed with flat-faced, watertight endcaps. Trajectories were obtained by recording the cylinder motion at 30 Hz using a CCD camera and extracting the displacement from the individual frames. The range of Reynolds numbers for these experiments was between 3800 and 9000.

To perform digital particle image velocimetry (DPIV), the flow was seeded with 14-micron silver coated glass spheres, which were illuminated by a thin light sheet from a 5 W continuous argon ion laser. Image pairs were acquired at 30 frame s^{-1} using a Kodak Megaplus CCD camera (1008×1018 pixels), and analysed using cross-correlation of subimages, with a two-step windowing process incorporating window shifting to determine particle displacements, and in turn, velocity fields. For the first correlation, interrogation windows of 64×64 pixels were used, with 32×32 pixel windows for the second correlation. Typical velocity fields comprised 60×60 velocity vectors, using a window overlap of 38 % in the second correlation.

The viewing area of the camera was 25.5 cm × 25.8 cm, with a corresponding time between images of 10 ms. The resulting vorticity fields were phase averaged over approximately 10 cycles from different experimental runs using the cylinder position as a reference, in order to remove small-scale turbulent fluctuations, but preserve the large-scale periodic structures. Further details pertaining to our implementation of the cross-correlation technique and to the level of particle seeding may be found in Govardhan & Williamson (2000).

The coordinate system is defined such that the transverse (Y) axis is horizontal and perpendicular to the cylinder's longitudinal (Z) axis, which is also horizontal, as shown in figure 5. The vertical streamwise (X) axis is positive in the direction opposite the mean velocity (upwards if falling, downwards if rising), so that in a reference frame moving at the mean velocity of the cylinder, positive X corresponds to the downstream direction. This ensures that the coordinate system is in accordance with convention for elastically mounted VIV experiments.

4. Critical mass for a freely rising XY cylinder

In the introduction, we presented a principal result coming from the preliminary paper by Horowitz & Williamson (2006), where it was shown that the critical mass for a rising or falling cylinder is close to 0.545. The Lissajous figures in figure 6, show very clearly the contrast in unsteady motion before the critical mass is reached ($m^* = 0.78$), and after the mass falls below this special value ($m^* = 0.45$). In addition to the large transverse amplitude ($A^*_Y \sim 1.0$) of the trajectory, the Lissajous plot for $m^* = 0.45$ shows substantial streamwise motion with an amplitude ($A^*_X \sim 0.3$). This streamwise vibration yields a figure-of-eight shape, in which the cylinder moves upstream as it reaches the peaks of its transverse motion. Figures 6(a) and 6(b) are plotted to the same scale to emphasize the striking change in the dynamics as the special critical mass is reached.

In studies of rising and falling bodies, it is common to characterize the system using the mass ratio, m^*, and the Galileo number, $Ga = \sqrt{|m^* - 1|gD^3}/\nu$ (Jenny *et al.* 2004). These quantities depend only on known parameters of the fluid and the body, and are independent of the resulting dynamics. In our experiments, as the masses of two cylinders ($D = 1.91, 2.54$ cm) were changed, the Galileo number would also vary as shown in figure 7(a). For each diameter, the mass ratio and Galileo number follow a curve in the $\{Ga, m^*\}$ plane, which may readily be determined from the definition of the Galileo number, where the values of the diameter, viscosity and gravity are held constant. For both cylinders, a jump from rectilinear motion (shown by open symbols) to periodic vibration (solid symbols) occurs when the mass ratio falls below $m^*_{crit} = 0.545 \pm 0.01$. This value of the critical mass appears to be valid in the range of Galileo numbers $Ga \approx 5000$–9000. The jump change in the dynamics is related to other studies, such as that by Jenny *et al.* (2004), and Horowitz & Williamson (2010), where in both cases, a critical relative density governs the regimes of vibration, for fixed Galileo number.

Since the Galileo number is undefined for elastically mounted systems, to which we wish to make comparisons, we also present our results in terms of the mass ratio and Reynolds number (figure 7b). The Reynolds number and the Galileo number are easily related through the drag coefficient C_D, according to $C_D = (\pi/2)(Ga/Re)^2$, for a cylinder.

The abrupt changes in dynamics we observe for rising cylinders are a phenomenon that has also been found in other studies of rising and falling bodies. In the case of

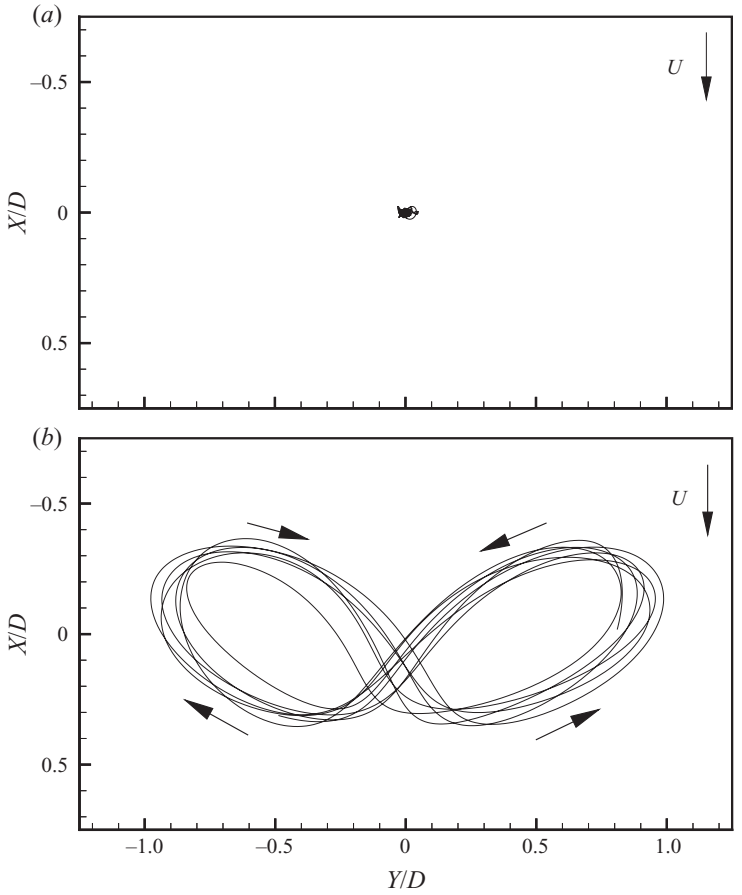

FIGURE 6. Lissajous figures for freely rising and falling cylinders. (*a*) $m^* = 0.78$, $Re = 5000$; cylinders with rectilinear trajectories show only small non-periodic motion in both transverse and streamwise directions. (*b*) $m^* = 0.45$, $Re = 3800$; rising cylinders vibrating in the transverse direction also exhibit significant streamwise oscillations ($A^*_X \approx 0.3$), producing a figure-of-eight shape.

spheres, for example, they have been observed by Jenny *et al.* (2004), and over a wide range of mass ratios and Galileo numbers by Horowitz & Williamson (2010). For other shapes, such as bubbles or short cylinders, the transitions in regimes of motion may also depend on the aspect ratio of the body (Mougin & Magnaudet 2002; Ern *et al.* 2007).

In the present study, the abrupt jump between the vibrating and rectilinear regimes of motion at the critical mass is illustrated by measurements of the amplitude as a function of the mass ratio, shown in figure 8, a subset of which appeared in Horowitz & Williamson (2006). This jump is evident in both the Y and X amplitudes, and for both cylinder diameters studied.

This critical mass for the rising and falling cylinder is remarkably close to the value found by Govardhan & Williamson (2002) for a Y-only cylinder, $m^*_{crit} = 0.542$, despite the significant amount of streamwise motion that is observed in the present experiments. However, we should note that the Y-only cylinder experiments are conducted at a Reynolds number, $Re = 22\,000$, whereas the present study near the

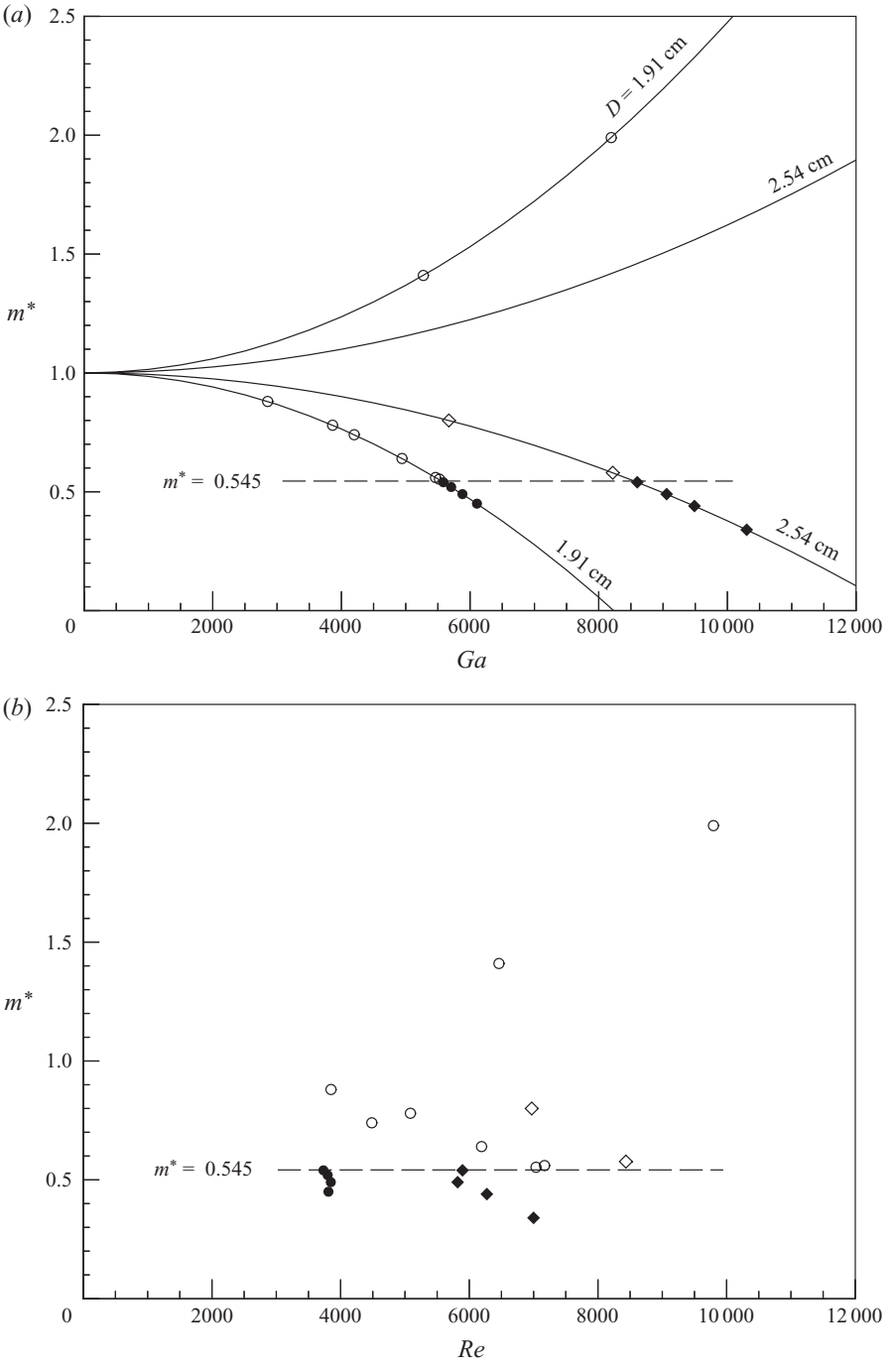

FIGURE 7. Rising cylinder dynamics in the (*a*) $\{Ga, m^*\}$ and (*b*) $\{Re, m^*\}$ planes. The cylinder dynamics jump from a rectilinear regime to large-amplitude vibration as $m^* = 0.545$ is crossed. ●, periodic vibration, $D = 1.91$ cm; ○, rectilinear motion, $D = 1.91$ cm; ◆, periodic vibration, $D = 2.54$ cm; ◇, rectilinear motion, $D = 2.54$ cm. The curves in (*a*) are determined from the definition of the Galileo number, for constant cylinder diameter and fluid properties.

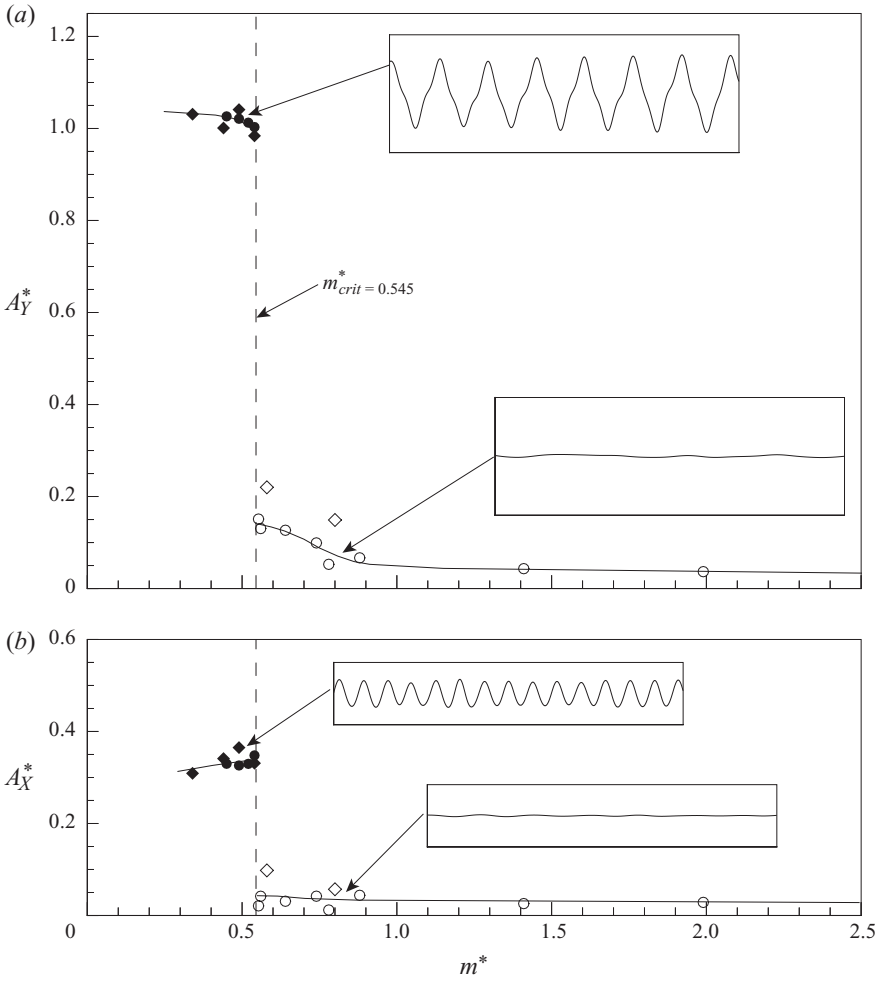

FIGURE 8. Existence of a critical mass for a rising cylinder. A sudden jump in the transverse and streamwise amplitudes occurs as the mass of the rising cylinder is reduced below a critical value of $m^*_{crit} = 0.545$. Time histories of X and Y displacement are plotted for mass ratios $m^* = 0.45$ and 0.78, showing the dramatic difference in the dynamics above and below the critical mass. ●, ○, $D = 1.91$ cm; ◆, ◇, $D = 2.54$ cm.

jump in amplitude in figure 8 is for $Re = 5000$. The work of Morse & Williamson (2009*a*) shows that the critical mass for a Y-only cylinder is influenced by Reynolds number; at $Re = 5000$, they find $m^*_{crit} = 0.4$. This is still reasonably similar to the critical mass found here for the rising cylinder, and we discuss these similarities later. We shall now characterize the dynamics of the rising body by examining its operating points and the corresponding modes of vortex formation.

5. Comparison between freely rising cylinders and elastically mounted cylinders

We plot the operating points for the rising cylinder in the frequency–amplitude $\{f_{v0}/f, A^*_Y\}$ plane in figure 9(*a*). At the highest mass ratios, the oscillations are desynchronized and almost negligible, occurring at a frequency equal to the vortex shedding frequency for a stationary cylinder ($f_{v0}/f = 1$). As the mass ratio is reduced,

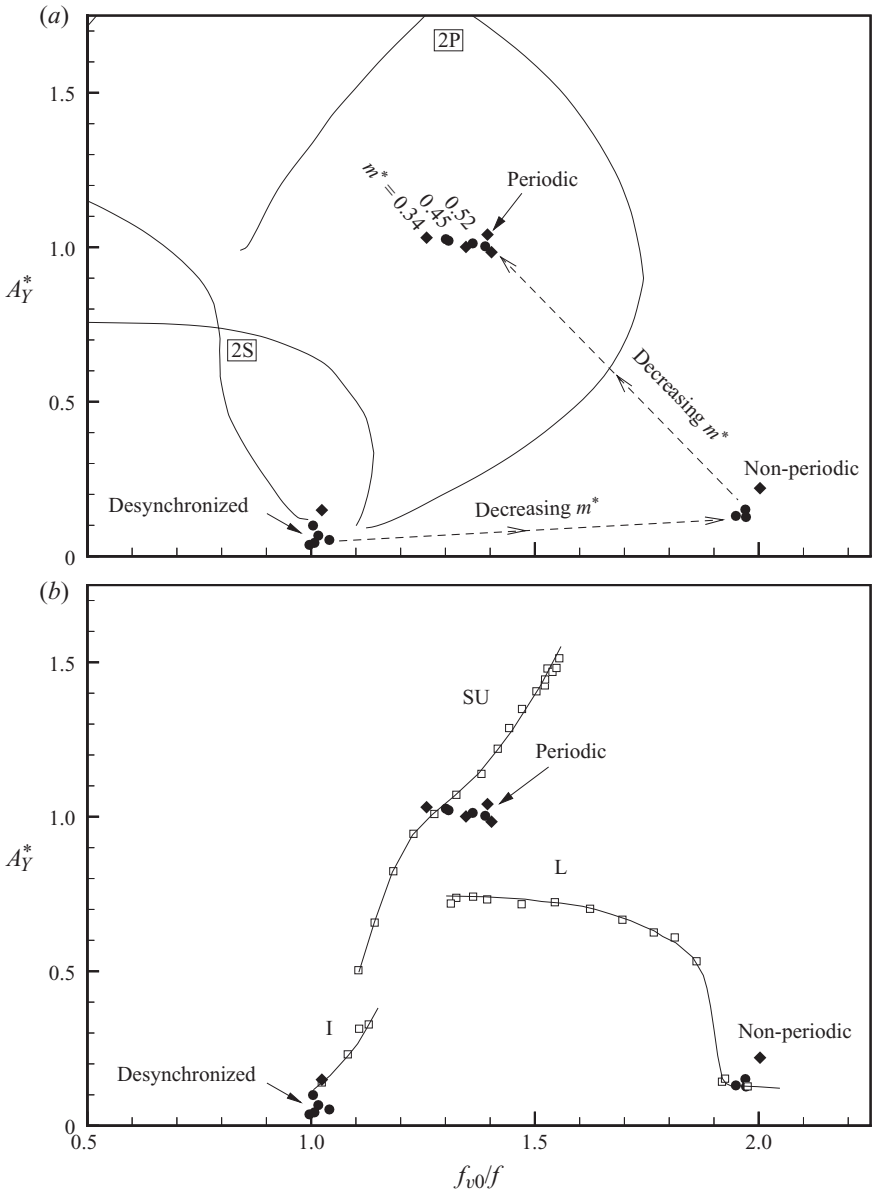

FIGURE 9. (*a*) Here we compare our operating point with the Williamson & Roshko (1988) map of wake modes (—) for an elastically mounted Y-only cylinder. We show the location of the operating point in the frequency–amplitude plane as m^* is decreased. For the highest mass ratios, the oscillations are desynchronized and almost negligible, while for mass ratios slightly above the critical value, small non-periodic oscillations occur. Below the critical mass, there is periodic vibration at high amplitude ($A_Y^* \sim 1$). (*b*) When compared with the elastically mounted XY cylinder, the operating point of the vibrating rising cylinder lies near the super-upper branch of response. ●, rising cylinder, $D = 1.91$ cm; ◆, rising cylinder, $D = 2.54$ cm; □, elastically mounted XY cylinder (Jauvtis & Williamson 2004).

but still slightly larger than the critical value, the cylinder undergoes low-amplitude non-periodic oscillations at about half the stationary shedding frequency. When the mass is reduced below the critical value, the sudden appearance of large-amplitude

periodic oscillations is accompanied by a jump in the frequency, placing the operating point at the centre of our plot in the amplitude–frequency plane in figure 9(*a*). On the basis of the wake dynamics for one d.o.f. *Y*-only cylinders, in the Williamson–Roshko map of regimes, this would suggest the presence of the 2P mode of vortex formation.

On the other hand, in figure 9(*b*), we see that the jump to periodic motion of the body places the operating point near the super-upper branch for an elastically mounted two degree-of-freedom *XY* cylinder. Given their close proximity, it is tempting to suggest that the freely rising cylinder might share some of the characteristics of the super-upper branch, found by Jauvtis & Williamson (2004), such as a 2T mode of vortex formation (comprising 2 vortex triplets per half cycle).

The operating points in figure 9 are plotted in the $\{f_{v0}/f, A_Y^*\}$ plane, and do not show the effect of streamwise motion or the phase angle. Lissajous plots of the rising cylinder as compared with an elastically mounted cylinder in the super-upper branch, shown in figures 10(*a*) and 10(*b*), reveal a marked difference: while the rising cylinder moves upstream at the transverse extrema of its motion, the elastically mounted cylinder moves downstream. This is equivalent to the two cases having the opposite phase between transverse and streamwise motion, with $\theta = 45^\circ$ for the rising cylinder, and $\theta = 225^\circ$ in the super-upper branch for the elastically mounted body. Judging by these results, one must suspect that the vortex dynamics will be quite different from the (*XY*) elastically mounted bodies.

At mass ratios above the critical value, where its trajectory is rectilinear, the cylinder exhibits a 2S mode of vortex formation, in the form of a Kármán street, as one might expect (Horowitz & Williamson 2006). On the other hand, the vibrating rising cylinder exhibits a classic 2P mode of vortex formation, comprising a pair of vortices each half cycle, shown in figure 2. The 2P mode is commonly found for cylinders constrained to move only transversely to the flow, and it is perhaps surprising to find this mode for a motion exhibiting significant streamwise vibration.

One may question how an *XY* system with significant streamwise motion is able to yield a similar critical mass (0.545) to that value found for bodies in transverse-only *Y* motion (0.4). We recall that in order for vibration to exist for a cylinder with zero damping and no restoring force, the following conditions must be satisfied: $C_Y \sin\phi = 0$, and $C_{EA} = -m^*$. The second condition requires that $\cos\phi < 0$, which corresponds to $\phi = 180^\circ$ for zero damping.

On the basis of previous free vibration experiments for both *Y*-only and *XY* cylinders, each vortex pattern is associated with a positive or negative effective added mass (C_{EA}), as follows:

$$\begin{aligned} &\text{2S Mode} \rightarrow C_{EA} > 0, \\ &\text{2P Mode} \rightarrow C_{EA} > 0, \quad \text{or} \quad C_{EA} < 0, \\ &\text{2T Mode} \rightarrow C_{EA} > 0. \end{aligned}$$

The existence of our vibration mode for the rising body is consistent with the fact that it exhibits the 2P mode, yielding $C_{EA} < 0$, corresponding to a positive cylinder mass. On the other hand, had the vortex pattern been the 2S or the 2T mode, we would find $C_{EA} > 0$, and vibration would not ensue. The above results suggest that, out of our set of modes {2S, 2P, 2T}, the 2P mode of vortex formation is the only vortex mode capable of causing VIV for a freely rising body! Of course, this does not preclude the existence of another mode, as yet undiscovered, causing vibrations of a rising cylinder.

For both the elastically mounted *Y* cylinder and the rising cylinder, the vortex modes are nearly identical (see figure 11), despite the presence of significant streamwise

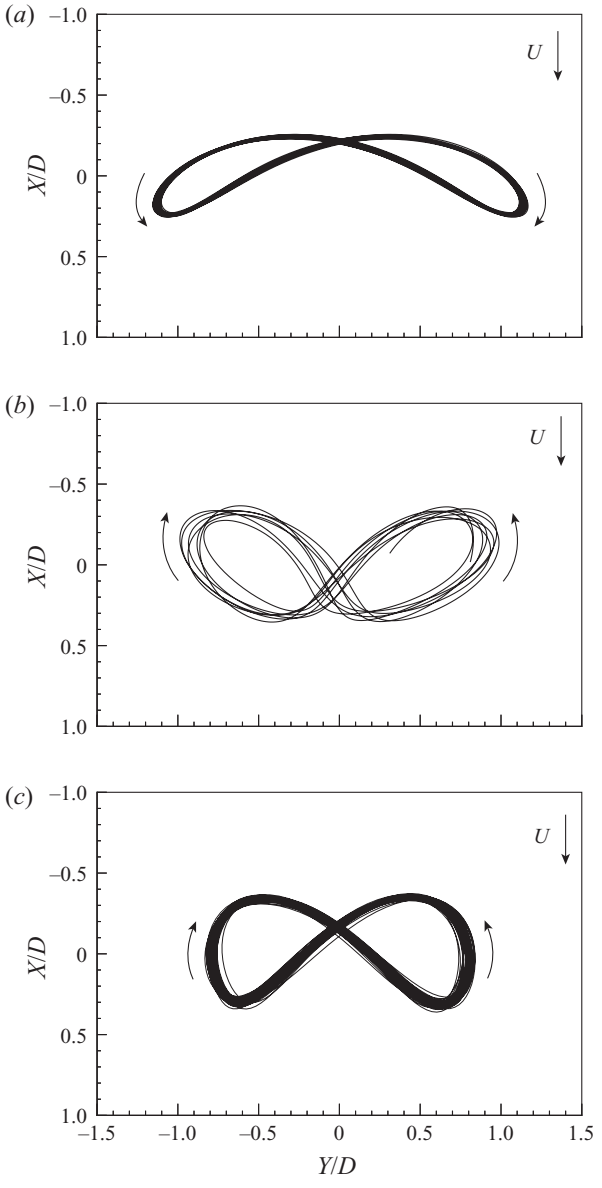

FIGURE 10. Lissajous figures and phase angles, θ, between X and Y motion. (a) Elastically mounted XY cylinder: $f_{NX} = f_{NY}$, $\theta = 225°$. (b) Freely rising cylinder: $m^* = 0.45$, $\theta = 45°$. (c) Elastically mounted XY cylinder: $f_{NX} = 2f_{NY}$, $\theta = -25°$, corresponding to an equivalent rising cylinder with $m^* = -C_{EA} = 0.48$.

motion for the rising body. Interestingly, one notes that the phase of vortex formation is also quite similar, which is consistent with a similar phase of vortex-induced force, capable of sustaining vibration. Measurement of the circulation strength of the vortices (at the instant when an entire shear layer of one sign is about to be shed, as in figure 11), yields $\Gamma^* = \Gamma/UD \sim 3.1$ for the stronger vortex in each pair, and $\Gamma^* \sim 1.7$ for the weaker vortex in the pair. These strengths are similar to those found by Govardhan & Williamson (2000) for the 2P mode for an elastically mounted

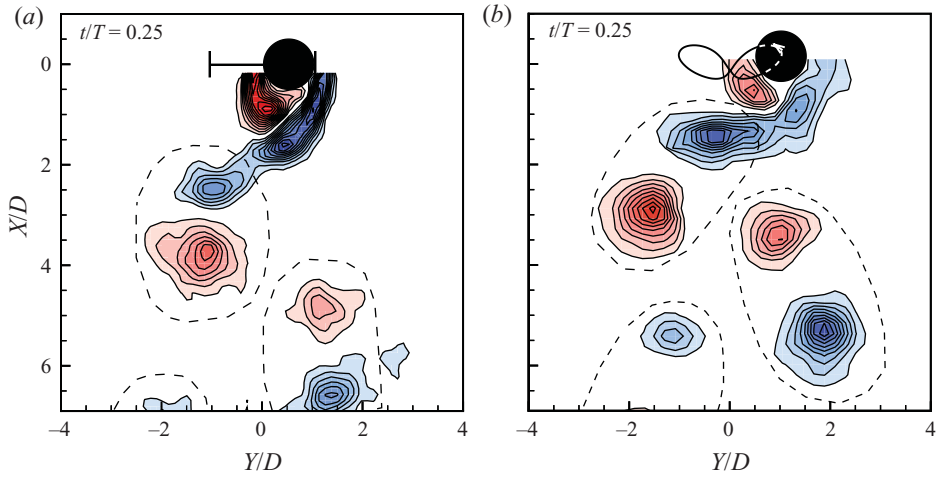

FIGURE 11. The 2P modes for (*a*) an elastically mounted Y-only cylinder, $A_X^* = 0$, $f_{v0}/f = 1.25$ and (*b*) a freely rising cylinder, $A_X^* = 0.32$, $f_{v0}/f = 1.55$. Although the rising cylinder has a significant streamwise amplitude, the vortex pattern is nearly unchanged from the Y-only case.

cylinder in the lower branch of response, corresponding to critical mass conditions for a Y-only cylinder (in which case, $\Gamma^* \sim 2.9$ and $\Gamma^* \sim 1.6$).

We may compute the force on the cylinder from a full knowledge of the body dynamics, employing the amplitude and frequency equations, following Khalak & Williamson (1999). For the rising cylinder, with zero stiffness and zero damping, the phase is $\phi = 180^\circ$ and the force is simply

$$C_Y = -C_{EA}\frac{2\pi^3 A^*}{(U^*/f^*)^2}, \tag{5.1}$$

where C_{EA} is known to be negative from the frequency equation, $m^* + C_{EA} = 0$.

This analysis assumes that the force and the displacement are sinusoidal, yet the time history of the transverse displacement shown in figure 12(*a*) contains components at higher frequencies, giving it a more sawtoothed shape. The effect of these higher frequencies on the force have been analysed by expressing the displacement using a Fourier series, as outlined the Appendix. The first 9 components of the Fourier series for the displacement have been used to construct the transverse force on the rising cylinder, shown in figure 12(*b*). The position spectrum in figure 12(*c*) shows that the two most significant frequencies are the f and $3f$ components, which appear prominently in the time history of the force. Such a $3f$ component has been found for other XY systems undergoing vibration (Jauvtis & Williamson 2004; Dahl *et al.* 2007). The $3f$ component of force is of comparable magnitude to the force at the fundamental frequency. However, it is the value of the effective added mass based on the fundamental frequency component of the force that will yield the critical mass, and the jump to large-amplitude vibration.

Comparisons of force magnitudes at the fundamental frequency (f) for the rising cylinder and for the Y-only cylinder indicate that similar values of critical mass are consistent with the similar values of amplitudes, frequencies and forces found between the two cases, despite the differences in the streamwise motion. Finally we comment on the almost identical critical mass for the rising body found here, as compared with the values found by Morse & Williamson (2009*a*) for high Reynolds number

Experiment	Re	Reference	m^*	C_{EA}	A^*	U^*/f^*	C_Y
Rising cylinder	4000	Present study	0.540	−0.540	0.82	6.86	0.58
Y-only cylinder, elastically mounted	10 000	Govardhan & Williamson (2000)	1.19	−0.551	0.68	6.15	0.62

TABLE 2. Force estimates from equations of motion for the rising cylinder and the elastically mounted, Y-only cylinder at similar A^* and U^*/f^*. When the rising cylinder is compared to an elastically mounted body at $Re = 10\,000$, for which the critical mass is similar, there is good agreement between the forces.

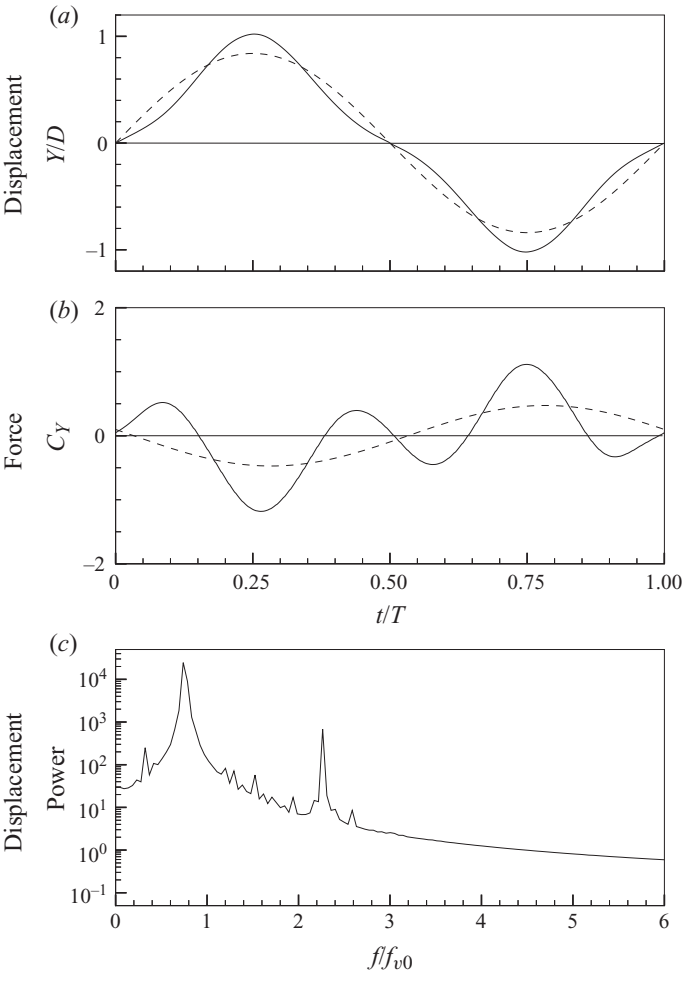

FIGURE 12. The non-sinusoidal shapes of the transverse displacement (a) and force (b) over a cycle are due to their $3f$ components, the strength of which is shown by the displacement spectrum (c). —, entire signal, including $3f$ component; - - -, fundamental frequency only.

($Re > 9000$). In table 2, we show some of the parameter values that together yield the $m^*_{crit} = 0.54$ for both the rising cylinder and the Y-motion cylinder at $Re = 10\,000$ from Govardhan & Williamson (2000). One of the parameters which seems to ensure agreement in the critical mass is the magnitude of the transverse force, which in turn

is related to the dynamics of the vortices and the strength of these vortices, all of which are quite similar for these two cases. Beyond noting the similarities in the vortex dynamics and induced forces above, it appears to be a coincidence that the rising body system, with its significant streamwise motion, yields comparable dynamics and forces sufficient to ensure such a good agreement in the critical mass.

6. Employing a special case of a two degree-of-freedom elastically mounted system to predict dynamics of rising or falling bodies

We have seen that it is not generally possible to use elastically mounted response data for an XY cylinder to determine the motion of an unrestrained body. Neither the approach of Jauvtis & Williamson (2004), where the natural frequencies in the streamwise and transverse directions are the same, nor that of Aronsen (2007), can be used to properly predict conditions at lower mass ratios, thereby to find the critical mass.

However, we now ask: is there any special case that can allow the motion of an unrestrained (rising) cylinder to be predicted from an elastically mounted response? For such a prediction to be possible, it is necessary that the amplitude and frequency response plots of elastically mounted systems collapse for different mass ratios. But, for the elastically mounted system we considered in § 2, the collapse of response data is not expected. We note that to make predictions of an unrestrained system, we must have $C_{EAX} = C_{EAY}$.

By examining the frequency equations, we may deduce a method of satisfying $C_{EAX} = C_{EAY}$ everywhere on an elastically mounted response. Then, each point on the response plot where the effective added mass is negative would correspond to the motion of an unrestrained cylinder with mass $m^* = -C_{EAY} = -C_{EAX}$. Since the frequencies of an XY system are given by

$$f_Y^* = \sqrt{\frac{m^* + C_A}{m^* + C_{EAY}}}, \quad f_X^* = \sqrt{\frac{m^* + C_A}{m^* + C_{EAX}}}, \tag{6.1}$$

it is clear that C_{EAY} and C_{EAX} can only be equal if $f_X^* = f_Y^*$. Recalling that the oscillation frequencies are related by $f_X = 2f_Y$, due to the symmetry of the forcing, we conclude that $f_X^* = f_Y^*$ will occur only when the streamwise natural frequency is twice the transverse natural frequency. In short, the system with natural frequencies arranged to be $f_{NX} = 2f_{NY}$, can predict the motions of unrestrained bodies at all mass ratios! Moreover, unlike the case with the same natural frequency in both directions, the response of systems with $f_{NX} = 2f_{NY}$ is expected to collapse for all mass ratios, provided that the mass-damping is close to zero.

Using the experimental apparatus described in Jauvtis & Williamson (2004), we performed experiments with a natural frequency ratio $f_{NX}/f_{NY} = 2.01$, for a mass ratio $m^* = 4.28$, and very low mass-damping, $(m^* + C_A)\zeta = 0.021$. The amplitude response of this system, shown in figure 13, exhibits three branches. An initial branch occurs over a very narrow range of flow velocities, corresponding to $U^* = 3.7$–4.0. This range of normalized velocity is small enough that a fine resolution in normalized velocity is needed to depict it accurately. From the initial branch to the upper branch, the amplitude drops before increasing again, producing a response with two peaks, the highest with an amplitude $A_Y^* \sim 1.0$ occurring at $Re = 5300$. Such a two-peaked response is qualitatively similar to the observations of Dahl *et al.* (2006) in experiments with a similar natural frequency ratio, $f_{NX}/f_{NY} = 1.9$. The upper branch also features a streamwise amplitude, up to $A_X^* = 0.35$, which is not insignificant relative to the

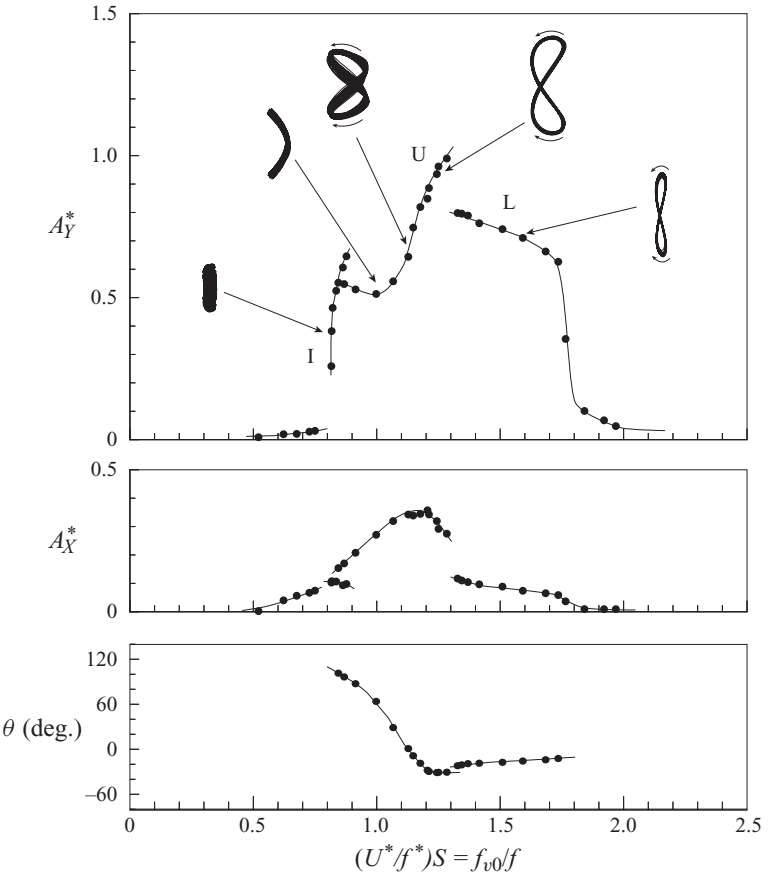

FIGURE 13. Special case of an elastically mounted XY cylinder where $f_{NX} = 2f_{NY}$. Response data and Lissajous figures are shown for $m^* = 4.28$. The synchronized response comprises a very narrow initial branch (I), an upper branch (U) with a large streamwise amplitude and a lower branch (L). The free stream for the Lissajous figures flows to the right. The phase θ is shown for the upper and lower branches only. $Re = 5300$ at peak amplitude, $(m^* + C_A)\zeta = 0.021$.

transverse motion, as seen in the Lissajous figures. The lower branch is very periodic, and has a small amount of streamwise motion ($A_X^* \sim 0.1$).

In the upper branch, the phase θ between the transverse and streamwise vibration, shown in figure 13(c), is between $-30°$ and $100°$, corresponding to the body moving upstream at its transverse peaks, the same qualitative behaviour as the freely rising cylinder ($\theta \sim 45°$). The Lissajous figures for these two cases are compared in figures 10(b) and 10(c). In these Lissajous plots, the elastically mounted response was chosen where $C_{EA} = -0.48$, which is expected to be equivalent to an unrestrained body with $m^* = 0.48$, and which is similar to the case of the rising cylinder ($m^* = 0.45$). The overall character of the motion for the rising body and the elastically mounted cylinder are quite similar.

By evaluating C_{EA} at each point in the synchronized response, we may evaluate a critical mass for an XY cylinder. As shown in figure 14, C_{EA} decreases throughout the upper branch, and reaches a maximum negative value for the synchronized regime in the lower branch. This value of C_{EA} is roughly constant throughout the lower branch, giving $m^*_{crit} = [-C_{EA}]_{max} = 0.57$ for $Re \sim 5500$–7000. The prediction of the critical mass

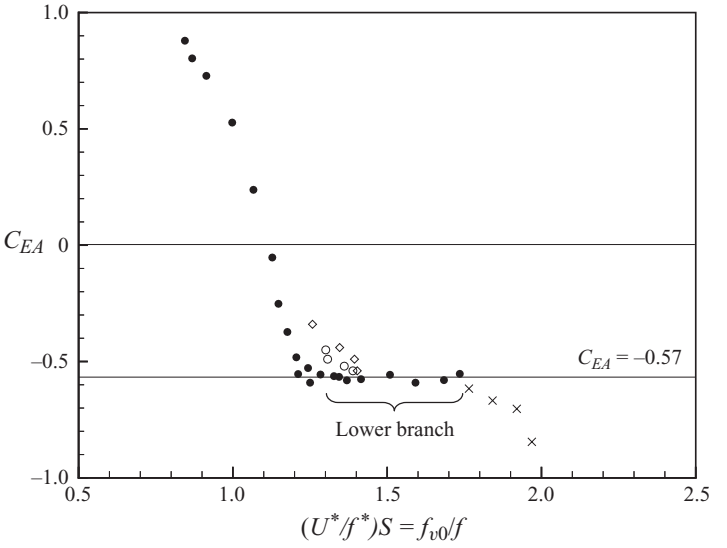

FIGURE 14. Values of C_{EA} for a cylinder with $f_{NX} = 2f_{NY}$. The maximum negative value of C_{EA}, corresponding to periodic vibration, occurs in the lower branch, yielding $m^*_{crit} = [-C_{EA}]_{max} \approx 0.57$, in good agreement with the critical mass measured for a freely rising cylinder, $m^*_{crit} = 0.545$. ●, elastically mounted cylinder, periodic vibration; ×, elastically mounted cylinder, desynchronized motion; ○, ◇, freely rising cylinders, $D = 1.91$ cm and $D = 2.54$ cm, $C_{EA} = -m^*$.

from the case of $f_{NX}/f_{NY} = 2$ agrees reasonably well with the value measured from the rising cylinder, $m^*_{crit} = 0.545$ ($Re = 5000$), and also with the experiments of Dahl *et al.* (2006), from whose data we may compute the value $m^*_{crit} = [-C_{EAY}]_{max} = 0.57$ for a cylinder with $f_{NX}/f_{NY} = 1.9$ at higher Reynolds number ($Re = 38\,000$).

Using the calculated values of C_{EA} and the corresponding response measurements for $f_{NX}/f_{NY} = 2$, we may predict the motion of freely rising cylinders with mass ratios $m^* = -C_{EA}$. From the amplitude measurements shown in figure 15, it is evident that the critical mass is predicted quite well. Interestingly, the trend found in the elastically mounted experiments is for the amplitude to decrease as mass is reduced, which is contrary to what one might imagine for bodies becoming very light. We may also use the response data to predict the XY dynamics of unrestrained bodies. These dynamics for 'equivalent' rising cylinders, whose mass ratios are given by $m^* = -C_{EA}$, are presented as Lissajous figures for several cases in figure 16.

The predictions of the motion of a freely rising cylinder described here were made using an elastically mounted system whose natural frequencies are $f_{NX} = 2f_{NY}$. But is it possible that we could find another natural frequency ratio that would also predict the dynamics of an unrestrained body? In general, the relationship between C_{EAX} and C_{EAY} for a system with an arbitrary ratio of natural frequencies is given by

$$C_{EAX} = \frac{1}{4}\left(\frac{f_{NX}}{f_{NY}}\right)^2 C_{EAY} - \left[1 - \frac{1}{4}\left(\frac{f_{NX}}{f_{NY}}\right)^2\right] m^*, \tag{6.2}$$

which may be derived from (6.1). Equation (6.2) will only satisfy the requirement for an unrestrained system, that $C_{EAX} = C_{EAY}$, when $f_{NX}/f_{NY} = 2$. Thus, we see that the case of a system with $f_{NX}/f_{NY} = 2$ is a special one, which is uniquely able to predict the response of a freely rising cylinder and the critical mass for an XY system.

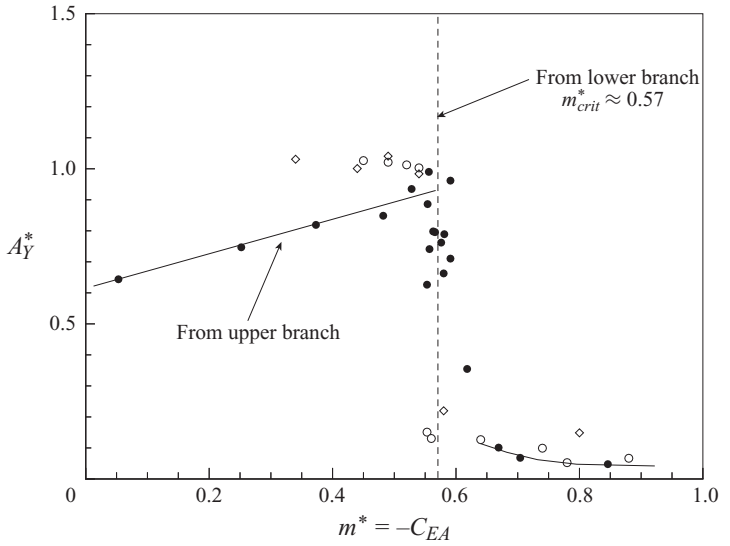

FIGURE 15. Predictions of amplitude for a freely rising cylinder using response data for an elastically mounted XY system with $f_{NX} = 2f_{NY}$. The amplitude is plotted for each point in the upper and lower branches where C_{EA} is negative, corresponding to a rising cylinder with mass $m^* = -C_{EA}$. ●, predictions from the elastically mounted response; ○, ◇, measured amplitude of freely rising cylinders, $D = 1.91$ cm and $D = 2.54$ cm.

7. Concluding remarks

Our original intent with this work was to investigate the existence of a critical mass for an elastically mounted cylinder with both transverse and streamwise d.o.f., by removing the spring restraints. However, such a study is not possible using conventional elastically mounted bodies, because the freedom to allow unrestrained motion in the streamwise direction would result in the body being carried away downstream by the flow! It turns out that a solution to this problem, which was considered initially, relevant to restrained vertically mounted cylinders, is to recognize that a freely rising or falling horizontal body is directly equivalent to a system having two d.o.f., with zero damping and spring stiffness. Of course, the fact that a rising body has no damping or stiffness, in itself, is a trivial statement, but here it allows us to connect the body of work on rising and falling bodies to elastically restrained systems, in particular enabling direct measurement of critical mass for restrained bodies.

In contrast with the case of a cylinder constrained to vibrate only in the transverse direction, the existence of a critical mass for an elastically mounted cylinder with two d.o.f. (and with the same natural frequency in both X and Y directions, $f_{NX} = f_{NY}$), cannot be predicted from response data from a single experiment at one mass ratio. This difficulty arises from the ability of streamwise vibration to yield different response branch shapes as the mass ratio is varied, even if the mass-damping parameter is kept constant.

The study of Horowitz & Williamson (2006) presented brief results directly related to the present work. The principal points stated in that paper, contained in a special issue related to a conference, are that there exists a critical mass of $m^*_{crit} = 0.545$, and that below this mass, the body vibrates vigorously as it rises, generating a 2P mode of vortex formation. In the present work, we discuss the fact that this value of critical

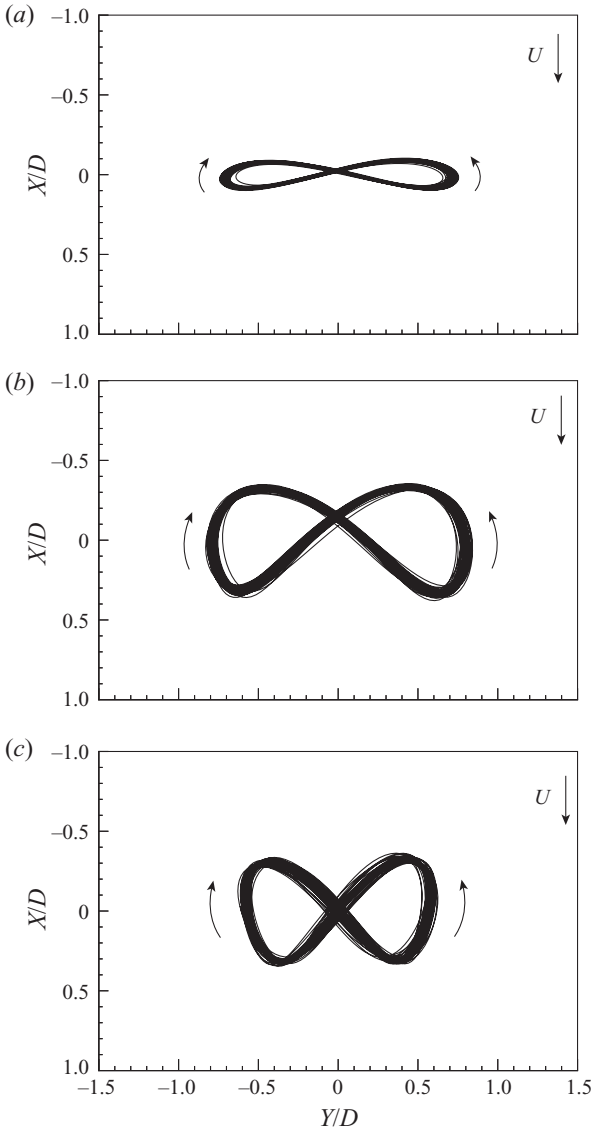

FIGURE 16. XY dynamics for 'equivalent' rising cylinders. The dynamics in these Lissajous figures for an elastically mounted system, with $f_{NX} = 2f_{NY}$, are expected to occur for rising cylinders, whose mass is given by $m^* = -C_{EA}$. (*a*) $m^* = 0.57$, (*b*) $m^* = 0.48$ and (*c*) $m^* = 0.06$.

mass is quite similar to the value measured when an elastically mounted cylinder is constrained to move only transverse to the flow (at the same Reynolds number), namely $m^*_{crit} = 0.4$, despite the presence of the significant streamwise motion for the rising body. The similarity in critical mass is related to the fact that we find direct similarities of the vortex wake configurations (the 2P mode), as well as similar vortex strengths, amplitudes and frequencies of body motion, which all lead to comparable values of the effective added mass (C_{EA}), and thereby to comparable critical masses for the two cases.

It should also be noted that the vortex formation is quite sensitive to the phase between streamwise and transverse motion, even for small streamwise amplitudes. In

the case of the rising cylinder, the phase of streamwise motion ($\theta = 45°$), illustrated by the Lissajous figures, appears to induce the 2P mode (in preference to the 2S or 2T modes). Such a phase angle exhibits an upstream movement when the body is at the transverse extrema, and represents a different mode than is found in any previous two degree-of-freedom system.

In this paper, we consider the existence of a periodic vibration mode for a freely rising cylinder, and deduce that it is caused by the fact that the 2P mode yields an effective added mass less than zero ($C_{EA} < 0$). If the vortex pattern had been the 2S or the 2T mode, found in other more restrained VIV studies, we would find $C_{EA} > 0$, and vibration for such a freely rising or falling body would not ensue (since it would be associated with a negative mass). This follows from the frequency equation for a freely rising body, which states that $m^* = -C_{EA}$. The above results suggest that, out of our set of previous VIV modes {2S, 2P, 2T}, the 2P mode of vortex formation is the only vortex mode capable of causing vortex-induced vibration for a rising body! As stated earlier in the paper, this does not preclude the existence of a mode, as yet undiscovered, causing vibrations of a freely rising cylinder.

Finally, we recognize that a two degree-of-freedom elastically mounted cylinder system can be devised where the effective added mass (C_{EA}) in the X and Y directions is precisely the same, meaning that, in the case where the springs are removed, the mass of the body is the same in the streamwise and transverse directions. This is obviously a condition that one has in a freely rising body. The only possible two degree-of-freedom elastically mounted cylinder system, which can be used to predict the dynamics of rising bodies, is one for which the natural frequencies in the streamwise (f_{NX}) and transverse (f_{NY}) directions are related by $f_{NX} = 2f_{NY}$. Such an arrangement may seem clear in retrospect, but it was not obvious at the outset that standard experiments, with equal orthogonal natural frequencies, would not be able to properly predict the critical mass, or the dynamics of a freely rising–falling cylinder.

Implementing such an elastic system, we are actually able to predict vibration amplitudes and critical mass ($m^*_{crit} = 0.57$) for a freely rising cylinder in reasonable agreement with direct measurements for such a rising body. We also predict the Lissajous figures representing the streamwise–transverse vibrations for a rising body with very small mass ratios (down to $m^* = 0.06$), which are unobtainable from our direct measurements. In this work, we find a critical 'relative density' for rising cylinders, which is consistent with predictions from elastically mounted experiments. Numerically, this critical mass is found to be 0.545, as mentioned earlier, and falls into the same regime as those values found for other VIV systems; for example, for rising spheres ($m^*_{crit} \approx 0.6$); for pivoted cylinders ($m^*_{crit} \approx 0.5$); Y only cylinders ($m^*_{crit} \approx 0.54$); XY cylinders ($m^*_{crit} \approx 0.57$). Although there is a distinct numerical similarity, it is not yet clear why these critical masses are so similar. We reiterate that critical mass is determined by the flow-induced forces, dictated by the complex vortex dynamics, so that understanding the clear similarity in critical mass across diverse systems requires consideration of the vortex forces, which are elusive to simple analytical expressions.

Appendix. Prediction of forces on a rising cylinder

The displacement of the rising cylinder contains components at frequencies higher than the fundamental, f. The effect of these higher frequency components on the

force may be analysed by expressing the displacement using a Fourier series

$$y(t) = \sum_{n=1}^{N} A_n \sin(n\omega t + \Phi_n), \tag{A 1}$$

where Φ_n is the phase between the nth component (at frequency $= nf$) and the fundamental component (frequency $= f$) obtained from a Fourier decomposition. For the component at the fundamental frequency, we have $\Phi_1 \equiv 0$. The force may be written as

$$F_Y(t) = \sum_{n=1}^{N} F_{Yn0} \sin(n\omega t + \phi_n + \Phi_n), \tag{A 2}$$

where ϕ_n is the phase between the force and displacement of the nth component. Taking advantage of orthogonality, (A 1) and (A 2) may be used to derive N-amplitude equations and N-frequency equations of the form

$$A_n^* = \frac{1}{4\pi^3} \frac{C_{Yn} \sin\phi_n}{(m* + C_A)\zeta} \left(\frac{U^*}{nf^*}\right)^2 nf^*, \tag{A 3}$$

$$nf^* = \sqrt{\frac{m^* + C_A}{m^* + C_{EAn}}}, \tag{A 4}$$

where

$$C_{EAn} = \frac{C_{Yn} \cos\phi_n}{2\pi^3 A_n^*} \left(\frac{U^*}{nf^*}\right)^2. \tag{A 5}$$

Equations (A 3) and (A 5) were used for the first nine components of the displacement (from f to $9f$) to calculate the transverse force on the rising cylinder, shown in figure 12(b). This analysis was performed on an average cycle of motion, calculated from all individual cycles for each of the experimental runs performed for $m^* = 0.45$ (a total of 22 cycles). The spectrum of the displacement in figure 12(c) shows that the two most significant frequencies are the f and $3f$ components, which appear prominently in the time history of the force in figure 12(b). Such a $3f$ component has been found for other XY systems undergoing vibration (Jauvtis & Williamson 2004; Dahl *et al.* 2007). The $3f$ component of force is of comparable magnitude to the force at the fundamental frequency. However, it is the value of the effective added mass based on the fundamental frequency component of the force that will yield the critical mass, and the jump to large-amplitude vibration.

REFERENCES

Aronsen, K. R. 2007 An experimental investigation of in-line and combined in-line and cross-flow vortex induced vibrations. PhD thesis, NTNU, Trondheim, Norway.

Bearman, P. 1984 Vortex shedding from oscillating bluff bodies. *J. Fluid Mech.* **16**, 195–222.

Clift, R., Grace, J. R. & Weber, M. E. 1973 *Bubbles, Drops, and Particles.* Academic.

Dahl, J. M., Hover, F. S. & Triantafyllou, M. S. 2006 Two-degree-of-freedom vortex-induced vibrations using a force assisted apparatus. *J. Fluids Struct.* **22**, 807–818.

Dahl, J. M., Hover, F. S., Triantafyllou, M. S., Dong, S. & Karniadakis, G. E. 2007 Resonant vibrations of bluff bodies cause multivortex shedding and high frequency forces. *Phys. Rev. Lett.* **99**, 144503.

Ern, P., Fernandes, P. C., Risso, F. & Magnaudet, J. 2007 Evolution of wake structure and wake-induced loads along the path of freely rising axisymmetric bodies. *Phys. Fluids* **19**, 113–302.

Feng, J., Hu, H. H. & Joseph, D. D. 1994 Direct simulation of initial value problems for the motion of solid bodies in a Newtonian fluid. Part 1. Sedimentation. *J. Fluid Mech.* **261**, 95–134.

Fernandes, P. C., Risso, F., Ern, P. & Magnaudet, J. 2007 Oscillatory motion and wake instability of freely rising axisymmetric bodies. *J. Fluid Mech.* **573**, 479–502.

Govardhan, R. & Williamson, C. H. K. 2000 Modes of vortex formation and frequency response of a freely vibrating cylinder. *J. Fluid Mech.* **420**, 85–130.

Govardhan, R. & Williamson, C. H. K. 2002 Resonance forever: existence of a critical mass and an infinite regime of resonance in vortex-induced vibration. *J. Fluid Mech.* **473**, 147–166.

Griffin, O. M. & Ramberg, S. E. 1982 Some recent studies of vortex shedding with application to marine tubulars and risers. *J. Energy Res. Tech.* **104**, 2–13.

Hartman, M. & Yates, J. G. 1993 Free-fall of solid particles through fluids. *Collect. Czech. Chem. Commun.* **58**, 961–982.

Horowitz, M. & Williamson, C. H. K. 2006 Dynamics of a rising and falling cylinder. *J. Fluids Struct.* **22**, 837–843.

Horowitz, M. & Williamson, C. H. K. 2008 Critical mass and a new periodic four-ring vortex wake mode for freely rising and falling spheres. *Phys. Fluids* **20**, 101–701.

Horowitz, M. & Williamson, C. H. K. 2010 The effect of Reynolds number on the dynamics and wakes of freely rising and falling spheres. *J. Fluid Mech.* **651**, 251–294.

Hover, F. S., Techet, A. H. & Triantafyllou, M. S. 1998 Forces on oscillating uniform and tapered cylinders in crossflow. *J. Fluid Mech.* **363**, 97–114.

Hu, H. H. 1995 Motion of a circular cylinder in a viscous liquid between parallel plates. *Theor. Comput. Fluid Dyn.* **363**, 441–455.

Isaacs, J. L. & Thodos, G. 1967 The free settling of solid cylindrical particles in the turbulent regime. *Can. J. Chem. Engng* **45**, 150–155.

Jauvtis, N. & Williamson, C. H. K. 2004 The effect of two degrees of freedom on vortex-induced vibration at low mass and damping. *J. Fluid Mech.* **509**, 23–62.

Jayaweera, K. O. L. F. & Mason, B. J. 1965 The behaviour of freely falling cylinders and cones in a viscous fluid. *J. Fluid Mech.* **22**, 709–720.

Jenny, M., Dušek, J. & Bouchet, G. 2004 Instabilities and transition of a sphere falling or ascending freely in a Newtonian fluid. *J. Fluid Mech.* **508**, 709–720.

Jeon, D. & Gharib, M. 2001 On circular cylinders undergoing two-degree-of-freedom forced motions. *J. Fluids Struct.* **15**, 533–541.

Jeon, D. & Gharib, M. 2004 On the relationship between the vortex formation process and cylinder wake vortex patterns. *J. Fluid Mech.* **519**, 161–181.

Khalak, A. & Williamson, C. H. K. 1999 Motions, forces and mode transitions in vortex-induced vibrations at low mass-damping. *J. Fluids Struct.* **10**, 813–851.

Magnaudet, J. & Eames, I. 2000 The motion of high Reynolds number bubbles in inhomogeneous flows. *Annu. Rev. Fluid Mech.* **32**, 659–708.

Marchildon, E. K., Clamen, A. & Gauvin, W. H. 1964 Drag and oscillatory motion of freely falling cylindrical particles. *Can. J. Chem. Engng* **42**, 178–182.

Moe, G. & Wu, Z.-J. 1990 The lift force on a cylinder vibrating in a current. *J. Offshore Mech. Arctic Engng* **112**, 297–303.

Morse, T. L. & Williamson, C. H. K. 2009*a* The effect of Reynolds number on the critical mass phenomenon in vortex-induced vibration. *Phys. Fluids* **21**, 045105.

Morse, T. L. & Williamson, C. H. K. 2009*b* Fluid forcing, wake modes, and transitions for a cylinder undergoing controlled oscillations. *J. Fluids Struct.* **25**, 697–712.

Morse, T. L. & Williamson, C. H. K. 2009*c* Prediction of vortex-induced vibration response by employing controlled motion. *J. Fluid Mech.* **634**, 5–39.

Mougin, G. & Magnaudet, J. 2002 Wake-induced forces and torques on a zigzagging/spiralling bubble. *Phys. Rev. Lett* **88**, 014502.

Parkinson, G. 1989 Phenomena and modelling of flow-induced vibrations of bluff bodies. *Prog. Aerosp. Sci.* **26**, 169–224.

Richardson, J. F. & Zaki, W. N. 1954 Sedimentation and fluidisation. Part I. *Trans. Inst. Chem. Engng* **32**, 35–53.

Sarpkaya, T. 1979 Vortex-induced oscillations. *J. Appl. Mech.* **46**, 241–258.

Sarpkaya, T. 1995 Hydrodynamic damping, flow-induced oscillations and biharmonic response. *J. Offshore Mech. Arctic Engng* **117**, 232–238.

Stringham, G. E., Simons, D. B. & Guy, H. P. 1969 The behavior of large particles falling in quiescent liquids. *Tech. Rep*. Paper 562C. US Geological Survey.

Veldhuis, C., Biesheuvel, A., van Wijngaarden, L. & Lohse, D. 2005 Motion and wake structure of spherical particles. *Nonlinearity* **18**, C1–C8.

Williamson, C. H. K. & Govardhan, R. N. 2004 Vortex-induced vibrations. *Annu. Rev. Fluid Mech.* **36**, 413–455.

Williamson, C. H. K. & Roshko, A. 1988 Vortex formation in the wake of an oscillating cylinder. *J. Fluids Struct*. **2**, 355–381.

Willmarth, W. W., Hawk, N. E. & Harvey, R. L. 1964 Steady and unsteady motions and wakes of freely falling disks. *Phys. Fluids* **7**, 197–208.